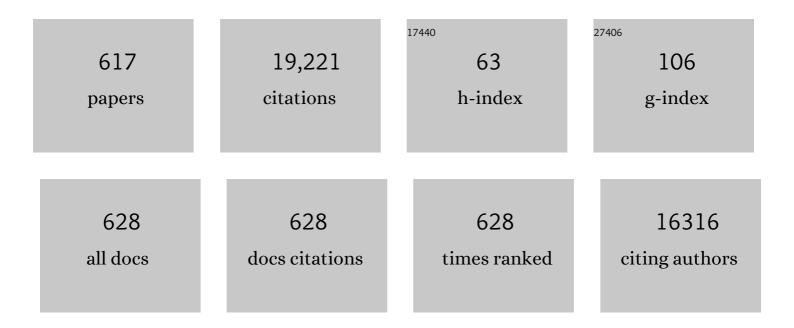
Yoshio Sakka

List of Publications by Year in descending order

Source: https://exaly.com/author-pdf/1608536/publications.pdf Version: 2024-02-01



YOSHIO SAKKA

#	Article	IF	CITATIONS
1	Green synthesis, structure feature and energy transfer of yellowâ€emitting (Y,Gd) ₂ O ₂ SO ₄ :Dy phosphors. Luminescence, 2022, 37, 199-207.	2.9	4
2	Fabrication of Textured Porous Ti ₃ SiC ₂ by Slip Casting under High Magnetic Field and Microstructural Evolution through High Temperature Deformation. Materials Transactions, 2022, 63, 133-140.	1.2	3
3	Auto-programmed synthesis of metallic aerogels: Core-shell Cu@Fe@Ni aerogels for efficient oxygen evolution reaction. Nano Energy, 2021, 81, 105644.	16.0	50
4	Elastic isotropy originating from heterogeneous interlayer elastic deformation in a Ti3SiC2 MAX phase with a nanolayered crystal structure. Journal of the European Ceramic Society, 2021, 41, 2278-2289.	5.7	7
5	Comparative Investigation on Upconversion Luminescence Properties of Lu 2 O 3 :Er/Yb and Lu 2 O 2 S:Er/Yb Phosphors. Physica Status Solidi (A) Applications and Materials Science, 2021, 218, 2100014.	1.8	3
6	Production of crystal-oriented lanthanum silicate oxyapatite ceramics with anisotropic electrical conductivity and thermal expansion. Open Ceramics, 2021, 6, 100100.	2.0	3
7	Fabrication of Textured Porous Ti ₃ SiC ₂ by Slip Casting under High Magnetic Field and Microstructural Evolution through High Temperature Deformation. Nippon Kinzoku Gakkaishi/Journal of the Japan Institute of Metals, 2021, 85, 256-263.	0.4	3
8	A mesoporous non-precious metal boride system: synthesis of mesoporous cobalt boride by strictly controlled chemical reduction. Chemical Science, 2020, 11, 791-796.	7.4	58
9	Amorphous Alloy Architectures in Pore Walls: Mesoporous Amorphous NiCoB Alloy Spheres with Controlled Compositions <i>via</i> a Chemical Reduction. ACS Nano, 2020, 14, 17224-17232.	14.6	46
10	New Development of Powder Processing under Eternal Fields. Funtai Oyobi Fummatsu Yakin/Journal of the Japan Society of Powder and Powder Metallurgy, 2020, 67, 47.	0.2	0
11	Fabrication Alumina Film with High Breakdown Field Strength by New Aerosol Gas Deposition Technology. Funtai Oyobi Fummatsu Yakin/Journal of the Japan Society of Powder and Powder Metallurgy, 2020, 67, 220-223.	0.2	0
12	Orientation Dependence of Plastic Deformation Behavior and Fracture Energy Absorption Mechanism around Vickers Indentation of Textured Ti ₃ SiC ₂ Sintered Body. Funtai Oyobi Fummatsu Yakin/Journal of the Japan Society of Powder and Powder Metallurgy, 2020, 67, 607-614.	0.2	1
13	Fabrication of Ceramics with Highly Controlled Microstructures by Advanced Fine Powder Processing. KONA Powder and Particle Journal, 2019, 36, 114-128.	1.7	7
14	Significantly improved photoluminescence of the greenâ€emitting βâ€sialon:Eu ²⁺ phosphor via surface coating of TiO ₂ . Journal of the American Ceramic Society, 2019, 102, 294-302.	3.8	5
15	Controlled Surface for Enhanced Luminescence Quantum Yields of Silicon Nanocrystals. Funtai Oyobi Fummatsu Yakin/Journal of the Japan Society of Powder and Powder Metallurgy, 2019, 66, 145-157.	0.2	1
16	Pulsed electrodischarged pressure sintering and flash sintering, a review. Materials Today: Proceedings, 2019, 16, 14-24.	1.8	7
17	Transparent magneto-optical Ho2O3 ceramics: Role of self-reactive resultant oxyfluoride additive and investigation of vacuum sintering kinetics. Ceramics International, 2019, 45, 14761-14767.	4.8	33
18	Heterocoagulation and SPS sintering of sulfonitric-treated CNT and 8YZ nanopowders. Journal of Asian Ceramic Societies, 2019, 7, 238-246.	2.3	4

#	Article	IF	CITATIONS
19	Preparation of Double-Shelled Fluorescent Silicon Nanocrystals and Fabrication of Its Thin Layer by Electrophoretic Deposition Process. Materials Transactions, 2019, 60, 49-54.	1.2	0
20	Photoluminescent and scintillant properties of highly transparent [(Y _{1â€} <i>_x</i> Gd <i>_x</i>) _{0.99} Dy _{0.01}] <sub (<i>xÂ</i>= 0 and 0.4) ceramics. Journal of the American Ceramic Society, 2019, 102, 4773-4780.</sub 	>2 <b susb>0	<sub7>3</sub7>
21	Development of Laser Optical Elements by Spark Plasma Sintering Technique. The Review of Laser Engineering, 2019, 47, 448.	0.0	0
22	Effect of texture on oxidation resistance of Ti3AlC2. Journal of the European Ceramic Society, 2018, 38, 3417-3423.	5.7	34
23	Inversion domain network stabilization and spinel phase suppression in ZnO. Journal of the American Ceramic Society, 2018, 101, 2616-2626.	3.8	9
24	Distribution of carbon contamination in oxide ceramics occurring during spark-plasma-sintering (SPS) processing: II - Effect of SPS and loading temperatures. Journal of the European Ceramic Society, 2018, 38, 2596-2604.	5.7	62
25	Photoluminescence efficiency significantly enhanced by surface modification of SiO2 coating on β-sialon:Eu2+ phosphor particle. Journal of Alloys and Compounds, 2018, 741, 454-458.	5.5	7
26	Stabilization of the high-temperature phase and total conductivity of yttrium-doped lanthanum germanate oxyapatite. Journal of the Ceramic Society of Japan, 2018, 126, 91-98.	1.1	3
27	Distribution of carbon contamination in MgAl2O4 spinel occurring during spark-plasma-sintering (SPS) processing: I – Effect of heating rate and post-annealing. Journal of the European Ceramic Society, 2018, 38, 2588-2595.	5.7	43
28	Transparent ultrafine Yb ³⁺ :Y ₂ O ₃ laser ceramics fabricated by spark plasma sintering. Journal of the American Ceramic Society, 2018, 101, 694-702.	3.8	37
29	Inherent anisotropy in transition metal diborides and microstructure/property tailoring in ultra-high temperature ceramics—A review. Journal of the European Ceramic Society, 2018, 38, 371-389.	5.7	89
30	Preparation of Double-shelled Fluorescent Silicon Nanocrystals and Fabrication of Its Thin Layer by Electrophoretic Deposition Process. Funtai Oyobi Fummatsu Yakin/Journal of the Japan Society of Powder and Powder Metallurgy, 2018, 65, 108-113.	0.2	0
31	Influence of the porosity caused by incomplete sintering on the mechanical behaviour of lanthanum silicate oxyapatite. Ceramics International, 2018, 44, 14348-14354.	4.8	6
32	Fabrication and Mechanical Properties of Textured Ti ₃ SiC ₂ Systems Using Commercial Powder. Materials Transactions, 2018, 59, 829-834.	1.2	10
33	Fabrication of Ceramics With Highly Controlled Microstructures by Advanced Powder Processing. , 2018, , 801-807.		Ο
34	Dense lanthanum silicate oxyapatite ceramics obtained by uniaxial pressing and slip casting. Science of Sintering, 2018, 50, 433-443.	1.4	0
35	High Performance of Ceramics and Manufacturing Process Innovation. Funtai Oyobi Fummatsu Yakin/Journal of the Japan Society of Powder and Powder Metallurgy, 2018, 65, 457.	0.2	0
36	Hydrothermal crystallization of a Ln ₂ (OH) ₄ SO ₄ ·nH ₂ O layered compound for a wide range of Ln (Ln = La–Dy), thermolysis, and facile transformation into oxysulfate and oxysulfide phosphors. RSC Advances, 2017, 7, 13331-13339.	3.6	31

Υοςηίο δάκκα

#	Article	IF	CITATIONS
37	Inversion domain boundaries in Mn and Al dualâ€doped ZnO: Atomic structure and electronic properties. Journal of the American Ceramic Society, 2017, 100, 4252-4262.	3.8	17
38	Photocatalytic growth of Ag nanocrystals on hydrothermally synthesized multiphasic TiO2/reduced graphene oxide (rGO) nanocomposites and their SERS performance. Applied Surface Science, 2017, 423, 1-12.	6.1	32
39	Yellow-emitting (Tb 1â^'x Ce x) 3 Al 5 O 12 phosphor powder and ceramic (0â‰ ¤ â‰ 0 .05): Phase evolution, photoluminescence, and the process of energy transfer. Ceramics International, 2017, 43, 8163-8170.	4.8	14
40	Dispersion and structural evolution of multi-walled carbon nanotubes in ZrB2 matrix. Ceramics International, 2017, 43, 10533-10539.	4.8	4
41	Interphase coordination design in carbamate-siloxane/vaterite composite microparticles towards tuning ion-releasing properties. Advanced Powder Technology, 2017, 28, 1349-1355.	4.1	4
42	Intensity of sulfonitric treatment on multiwall carbon nanotubes. Chemical Physics Letters, 2017, 689, 135-141.	2.6	21
43	Preparation of carbamate-containing vaterite particles for strontium removal in wastewater treatment. Journal of Asian Ceramic Societies, 2017, 5, 364-369.	2.3	6
44	EDTA-assisted phase conversion synthesis of (Gd _{0.95} RE _{0.05})PO ₄ nanowires (RE = Eu, Tb) and investigation of photoluminescence. Science and Technology of Advanced Materials, 2017, 18, 447-457.	6.1	10
45	Highâ€ŧemperature strength and plastic deformation behavior of niobium diboride consolidated by spark plasma sintering. Journal of the American Ceramic Society, 2017, 100, 5295-5305.	3.8	22
46	Effect of texture microstructure on tribological properties of tailored Ti3AlC2 ceramic. Journal of Advanced Ceramics, 2017, 6, 120-128.	17.4	25
47	Ultra-high elevated temperature strength of TiB2-based ceramics consolidated by spark plasma sintering. Journal of the European Ceramic Society, 2017, 37, 393-397.	5.7	51
48	Fabrication and Mechanical Properties of Textured Ti ₃ SiC ₂ Systems Using Commercial Powders. Funtai Oyobi Fummatsu Yakin/Journal of the Japan Society of Powder and Powder Metallurgy, 2017, 64, 552-557.	0.2	0
49	Possibility of Low-Temperature High-Strain-Rate Superplasticity in Fine-Grained Ceramic Materials. Funtai Oyobi Fummatsu Yakin/Journal of the Japan Society of Powder and Powder Metallurgy, 2017, 64, 515-522.	0.2	0
50	Spark Plasma Sintering of Highly Transparent Hydroxyapatite Ceramics. Funtai Oyobi Fummatsu Yakin/Journal of the Japan Society of Powder and Powder Metallurgy, 2017, 64, 547-551.	0.2	12
51	Effects of Pretreatment of Source Powder Mixture on Aerosol Gas Deposition Film Synthesis and Luminescence. Funtai Oyobi Fummatsu Yakin/Journal of the Japan Society of Powder and Powder Metallurgy, 2017, 64, 558-562.	0.2	1
52	Development of powder processing under external fields. Funtai Oyobi Fummatsu Yakin/Journal of the Japan Society of Powder and Powder Metallurgy, 2016, 63, 793.	0.2	0
53	Preparation of Gallium Stannate Dense Sintered Body Using SPS Method. Funtai Oyobi Fummatsu Yakin/Journal of the Japan Society of Powder and Powder Metallurgy, 2016, 63, 986-989.	0.2	0
54	Synthesis of crystallographically oriented olivine aggregates using colloidal processing in a strong magnetic field. Physics and Chemistry of Minerals, 2016, 43, 689-706.	0.8	2

#	Article	IF	CITATIONS
55	Electrophoretic fabrication of a-b plane oriented La2NiO4 cathode onto electrolyte in strong magnetic field for low-temperature operating solid oxide fuel cell. Journal of the European Ceramic Society, 2016, 36, 4077-4082.	5.7	19
56	Highâ€Temperature Strength of Boron Suboxide Ceramic Consolidated by Spark Plasma Sintering. Journal of the American Ceramic Society, 2016, 99, 2769-2777.	3.8	13
57	Triaxial Crystalline Orientation of MgTi ₂ O ₅ Achieved Using a Strong Magnetic Field and Geometric Effect. Journal of the American Ceramic Society, 2016, 99, 1852-1854.	3.8	7
58	High‣trength B ₄ C–TaB ₂ Eutectic Composites Obtained via <i>In Situ</i> by Spark Plasma Sintering. Journal of the American Ceramic Society, 2016, 99, 2436-2441.	3.8	24
59	Synthesis of iron oxide nanoparticles with different morphologies by precipitation method with and without chitosan addition. Journal of the Ceramic Society of Japan, 2016, 124, 489-494.	1.1	12
60	Microstructural analysis and thermoelectric properties of Sn-Al co-doped ZnO ceramics. AIP Conference Proceedings, 2016, , .	0.4	6
61	Prevention of thermal- and moisture-induced degradation of the photoluminescence properties of the Sr ₂ Si ₅ N ₈ :Eu ²⁺ red phosphor by thermal post-treatment in N ₂ –H ₂ . Physical Chemistry Chemical Physics, 2016, 18, 12494-12504.	2.8	36
62	Flash spark plasma sintering of ultrafine yttria-stabilized zirconia ceramics. Scripta Materialia, 2016, 121, 32-36.	5.2	46
63	Surface modification of multiwall carbon nanotubes by sulfonitric treatment. Applied Surface Science, 2016, 379, 264-269.	6.1	89
64	Electrophoretic deposition for obtaining dense lanthanum silicate oxyapatite (LSO). Ceramics International, 2016, 42, 19283-19288.	4.8	11
65	Columnar and DVC-structured thermal barrier coatings deposited by suspension plasma spray: high-temperature stability and their corrosion resistance to the molten salt. Ceramics International, 2016, 42, 16822-16832.	4.8	20
66	Development of an electrochemical impedance analysis program based on the expanded measurement model. Journal of the Ceramic Society of Japan, 2016, 124, 943-949.	1.1	18
67	Sintering characteristics and thermoelectric properties of Mn–Al co-doped ZnO ceramics. Journal of the Ceramic Society of Japan, 2016, 124, 515-522.	1.1	22
68	High temperature flexural strength in monolithic boron carbide ceramic obtained from two different raw powders by spark plasma sintering. Journal of the Ceramic Society of Japan, 2016, 124, 587-592.	1.1	13
69	Low-temperature spark plasma sintering of alumina by using SiC molding set. Journal of the Ceramic Society of Japan, 2016, 124, 1141-1145.	1.1	12
70	Effects of Processing Parameters on the Deposition of Yttria Partially Stabilized Zirconia Coating During Suspension Plasma Spray. Journal of the American Ceramic Society, 2016, 99, 3546-3555.	3.8	22
71	Highly Segmented Thermal Barrier Coatings Deposited by Suspension Plasma Spray: Effects of Spray Process on Microstructure. Journal of Thermal Spray Technology, 2016, 25, 1638-1649.	3.1	13
72	Fabrication and Mechanical Properties of Textured Ti ₃ SiC ₂ MAX Phase Systems. Funtai Oyobi Fummatsu Yakin/Journal of the Japan Society of Powder and Powder Metallurgy, 2016, 63, 970-975.	0.2	2

#	Article	lF	CITATIONS
73	Dispersion and Reinforcing Mechanism of Carbon Nanotubes in a Ceramic Material. Funtai Oyobi Fummatsu Yakin/Journal of the Japan Society of Powder and Powder Metallurgy, 2016, 63, 955-964.	0.2	2
74	Fabrication of Dense Nanostructured Bulk Ceramics by Means of Spark-Plasma-Sintering (SPS) Processing. Materials Science Forum, 2016, 838-839, 225-230.	0.3	1
75	Reduction in sintering temperature for flash-sintering of yttria by nickel cation-doping. Acta Materialia, 2016, 106, 344-352.	7.9	64
76	Magnetic field alignment in highly concentrated suspensions for gelcasting process. Ceramics International, 2016, 42, 294-301.	4.8	6
77	Hardness and toughness control of brittle boron suboxide ceramics by consolidation of star-shaped particles by spark plasma sintering. Ceramics International, 2016, 42, 3525-3530.	4.8	13
78	Densification kinetics during isothermal sintering of 8YSZ. Journal of the European Ceramic Society, 2016, 36, 1269-1275.	5.7	22
79	Improved galvanic replacement growth of Ag microstructures on Cu micro-grid for enhanced SERS detection of organic molecules. Materials Science and Engineering C, 2016, 61, 97-104.	7.3	13
80	Influence of pre- and post-annealing on discoloration of MgAl2O4 spinel fabricated by spark-plasma-sintering (SPS). Journal of the European Ceramic Society, 2016, 36, 2961-2968.	5.7	49
81	High-strength TiB 2 –TaC ceramic composites prepared using reactive spark plasma consolidation. Ceramics International, 2016, 42, 1298-1306.	4.8	48
82	Fabrication, microstructure and properties of in situ synthesized B4C^ ^ndash;NbB2 eutectic composites by spark plasma sintering. Journal of the Ceramic Society of Japan, 2015, 123, 33-37.	1.1	20
83	Deflocculation and stabilization of Ti ₃ SiC ₂ ceramic powder in gelcasting process. Journal of the Ceramic Society of Japan, 2015, 123, 1010-1017.	1.1	12
84	Consolidation of B ₄ C–VB ₂ eutectic ceramics by spark plasma sintering. Journal of the Ceramic Society of Japan, 2015, 123, 1051-1054.	1.1	9
85	Sinterable powder fabrication of lanthanum silicate oxyapatite based on solid-state reaction method. Journal of the Ceramic Society of Japan, 2015, 123, 274-279.	1.1	8
86	Nano ZrO ₂ –TiN composites with high strength and conductivity. Journal of the Ceramic Society of Japan, 2015, 123, 86-89.	1.1	6
87	Assessment of carbon contamination in MgAl ₂ 0 ₄ spinel during spark-plasma-sintering (SPS) processing. Journal of the Ceramic Society of Japan, 2015, 123, 983-988.	1.1	37
88	Effects of High Magnetic Fields on Thermal Convection Using Feeble Magnetic Conductive Aqueous Solutions. Bulletin of the Chemical Society of Japan, 2015, 88, 1404-1409.	3.2	0
89	Synthesis of <i>Multilayered</i> Starâ€Shaped B ₆ O Particles Using the Seedâ€Mediated Growth Method. Journal of the American Ceramic Society, 2015, 98, 3635-3638.	3.8	14
90	Fabrication of (111)-oriented Tetragonal BaTiO ₃ Ceramics by an Electrophoretic Deposition in a High Magnetic Field. Transactions of the Materials Research Society of Japan, 2015, 40, 223-226.	0.2	8

Υοςηίο δάκκα

#	Article	IF	CITATIONS
91	Fabrication and Characterization of Transparent (Y _{0.98â^'<i>x</i>} Tb _{0.02} Eu _{<i>x</i>}) ₂ O ₃ Ceramics with Colorâ€Tailorable Emission. Journal of the American Ceramic Society, 2015, 98, 3877-3883.	3.8	13
92	Recent progress in advanced optical materials based on gadolinium aluminate garnet (Gd ₃ Al ₅ O ₁₂). Science and Technology of Advanced Materials, 2015, 16, 014902.	6.1	90
93	High-temperature reactive spark plasma consolidation of TiB2–NbC ceramic composites. Ceramics International, 2015, 41, 10828-10834.	4.8	52
94	Processing and enhanced piezoelectric properties of highly oriented compositionally modified Pb(Zr,Ti)O ₃ ceramics fabricated by magnetic alignment. Applied Physics Express, 2015, 8, 041501.	2.4	8
95	Consolidation of B4C-TaB2 eutectic composites by spark plasma sintering. Journal of Asian Ceramic Societies, 2015, 3, 369-372.	2.3	18
96	Influence of Spark Plasma Sintering (<scp>SPS</scp>) Conditions on Transmission of MgAl ₂ O ₄ Spinel. Journal of the American Ceramic Society, 2015, 98, 378-385.	3.8	44
97	Controlled Synthesis of Layered Rareâ€Earth Hydroxide Nanosheets Leading to Highly Transparent (Y _{0.95} Eu _{0.05}) ₂ O ₃ Ceramics. Journal of the American Ceramic Society, 2015, 98, 1413-1422.	3.8	32
98	Facile and green production of aqueous graphene dispersions for biomedical applications. Nanoscale, 2015, 7, 6436-6443.	5.6	114
99	Highly anisotropic single crystal-like La2Ti2O7 ceramic produced by combined magnetic field alignment and templated grain growth. Journal of the European Ceramic Society, 2015, 35, 1771-1776.	5.7	20
100	Densification, microstructure evolution and mechanical properties of WC doped HfB2–SiC ceramics. Journal of the European Ceramic Society, 2015, 35, 2707-2714.	5.7	37
101	Photoluminescent and cathodoluminescent performances of Tb ³⁺ in Lu ³⁺ -stabilized gadolinium aluminate garnet solid-solutions of [(Gd _{1â^'x} Lu _x) _{1â^'y} Tb _y] ₃ Al ₅ O _{ RSC Advances, 2015, 5, 59686-59695.}	> 326	.17
102	Effects of high magnetic fields on thermal convection of conductive aqueous solution. Japanese Journal of Applied Physics, 2015, 54, 077301.	1.5	2
103	One-step freezing temperature crystallization of layered rare-earth hydroxide (Ln ₂ (OH) ₅ NO ₃ ·nH ₂ O) nanosheets for a wide spectrum of Ln (Ln = Pr–Er, and Y), anion exchange with fluorine and sulfate, and microscopic coordination probed via photoluminescence. Journal of Materials Chemistry C. 2015, 3, 3428-3437.	5.5	50
104	Influence of the crystal structure on the physical properties of monoclinic ZrO 2 nanocrystals. Nano Structures Nano Objects, 2015, 1, 1-6.	3.5	3
105	45S5 Bioglass®–MWCNT composite: processing and bioactivity. Journal of Materials Science: Materials in Medicine, 2015, 26, 199.	3.6	26
106	Reduced thermal degradation of the red-emitting Sr ₂ Si ₅ N ₈ :Eu ²⁺ phosphor via thermal treatment in nitrogen. Journal of Materials Chemistry C, 2015, 3, 7642-7651.	5.5	60
107	Room-temperature synthesis of Bi ₄ Ge ₃ O ₁₂ from aqueous solution. Japanese Journal of Applied Physics, 2015, 54, 06FJ03.	1.5	7
108	Effects of Gd Substitution on Sintering and Optical Properties of Highly Transparent (Y _{0.95â^'<i>x</i>} Gd _{<i>x</i>} Eu _{0.05}) ₂ O ₃ Ceramics. Journal of the American Ceramic Society, 2015, 98, 2480-2487.	3.8	31

#	Article	IF	CITATIONS
109	Research and Development of the Coprecipitation Process for Lanthanum Germanate Oxyapatite. Journal of the American Ceramic Society, 2015, 98, 66-70.	3.8	6
110	Synthesis of Highly Photocatalytic TiO ₂ Microflowers Based on Solvothermal Approach Using <i>N,N</i> -Dimethylformamide. Journal of Nanoscience and Nanotechnology, 2015, 15, 4747-4751.	0.9	18
111	Spectroscopic study of the discoloration of transparent MgAl2O4 spinel fabricated by spark-plasma-sintering (SPS) processing. Acta Materialia, 2015, 84, 9-19.	7.9	88
112	Sinterable Powder Fabrication and the Oxygen-ion Conductivity of Lanthanum Silicate Oxyapatite. Journal of the Society of Powder Technology, Japan, 2015, 52, 648-657.	0.1	0
113	Fabrication of Textured Ti2AlN Ceramic by Slip Casting in a Strong Magnetic Field and Spark Plasma Sintering. Funtai Oyobi Fummatsu Yakin/Journal of the Japan Society of Powder and Powder Metallurgy, 2014, 61, 538-543.	0.2	6
114	Challenges of nanostructuring and functional properties for selected bulk materials obtained by reactive spark plasma sintering. Japanese Journal of Applied Physics, 2014, 53, 05FB22.	1.5	9
115	Recent advances in understanding the reinforcing ability and mechanism of carbon nanotubes in ceramic matrix composites. Science and Technology of Advanced Materials, 2014, 15, 064902.	6.1	73
116	Tens of micron-sized unilamellar nanosheets of Y/Eu layered rare-earth hydroxide: efficient exfoliation via fast anion exchange and their self-assembly into oriented oxide film with enhanced photoluminescence. Science and Technology of Advanced Materials, 2014, 15, 014203.	6.1	42
117	<i>In Situ</i> Observation of Diamagnetic Fluid Flow in High Magnetic Fields. Key Engineering Materials, 2014, 616, 188-193.	0.4	1
118	Phosphor Deposits of β-Sialon:Eu2+ Mixed with SnO2 Nanoparticles Fabricated by the Electrophoretic Deposition (EPD) Process. Materials, 2014, 7, 3623-3633.	2.9	11
119	Reductant-Free Colloidal Synthesis of Near-IR Emitting Germanium Nanocrystals: Role of Primary Amine. Journal of Nanoscience and Nanotechnology, 2014, 14, 2204-2210.	0.9	5
120	Trends in electronic structures and structural properties of MAX phases: a first-principles study on M ₂ AlC (M = Sc, Ti, Cr, Zr, Nb, Mo, Hf, or Ta), M ₂ AlN, and hypothetical M ₂ AlB phases. Journal of Physics Condensed Matter, 2014, 26, 505503.	1.8	116
121	Facile and green synthesis of (La _{0.95} Eu _{0.05}) ₂ O ₂ S red phosphors with sulfate-ion pillared layered hydroxides as a new type of precursor: controlled hydrothermal processing, phase evolution and photoluminescence. Science and Technology of Advanced Materials, 2014, 15, 014204.	6.1	23
122	Effective Use of Mesoporous Silica Filler: Comparative Study on Thermal Stability and Transparency of Silicone Rubbers Loaded with Various Kinds of Silica Particles. European Journal of Inorganic Chemistry, 2014, 2014, 2773-2778.	2.0	24
123	Microwave Sintering of <scp><scp>Ti</scp></scp> ₃ <scp><scp>Si</scp>(<scp>(<scp>Al</scp></scp>)<scp>Ceramic. Journal of the American Ceramic Society, 2014, 97, 2731-2735.</scp></scp>	:a> <td>cp16sub>2<</td>	cp 16 sub>2<
124	Hybrid White Light Emitting Diode Based on Silicon Nanocrystals. Advanced Functional Materials, 2014, 24, 7151-7160.	14.9	63
125	Particle processing technology. Science and Technology of Advanced Materials, 2014, 15, 010201.	6.1	0
126	Mechanically reliable thermoelectric (TE) nanocomposites by dispersing and embedding TE-nanostructures inside a tetragonal ZrO2matrix: the concept and experimental demonstration in graphene oxide–3YSZ system. Science and Technology of Advanced Materials, 2014, 15, 014201.	6.1	14

#	Article	IF	CITATIONS
127	Crystalline-Oriented Beta-Sialon:Eu2+Deposits Fabricated by Electrophoretic Deposition (EPD) within Strong Magnetic Field. ECS Journal of Solid State Science and Technology, 2014, 3, R195-R199.	1.8	2
128	Research progress in nondoped lanthanoid silicate oxyapatites as new oxygen-ion conductors. Journal of the Ceramic Society of Japan, 2014, 122, 921-939.	1.1	25
129	Rudimental research progress of rare-earth silicate oxyapatites: their identification as a new compound until discovery of their oxygen ion conductivity. Journal of the Ceramic Society of Japan, 2014, 122, 649-663.	1.1	22
130	MOF-derived Nanoporous Carbon as Intracellular Drug Delivery Carriers. Chemistry Letters, 2014, 43, 717-719.	1.3	165
131	Microstructure and high-temperature strength of textured and non-textured ZrB ₂ ceramics. Science and Technology of Advanced Materials, 2014, 15, 014202.	6.1	43
132	A strategy for fabricating textured silicon nitride with enhanced thermal conductivity. Journal of the European Ceramic Society, 2014, 34, 2585-2589.	5.7	53
133	Synthesis, characterization, and photoluminescent properties of (La0.95Eu0.05)2O2SO4 red phosphors with layered hydroxyl sulfate as precursor. Journal of Alloys and Compounds, 2014, 603, 28-34.	5.5	17
134	Thermal Conversion of Hollow Prussian Blue Nanoparticles into Nanoporous Iron Oxides with Crystallized Hematite Phase. European Journal of Inorganic Chemistry, 2014, 2014, 1137-1141.	2.0	27
135	Microstructure and <scp>A</scp> nisotropic <scp>P</scp> roperties of <scp>T</scp> extured <scp>Z</scp> r <scp>B</scp> ₂ and <scp>Z</scp> r <scp>B</scp> ₂ â€" <scp>M</scp> o <scp>S</scp> i ₂ Â <scp>C</scp> erami <scp>P</scp> repared by <scp>S</scp> trong <scp>M</scp> agnetic <scp>F</scp> ield	C 2. 1	22
136	In Situ TEM Observation of a Microcrucible Mechanism of Nanowire Growth. Science, 2014, 344, 623-626.	12.6	58
137	Beta-sialon phosphor deposits fabricated by electrophoretic deposition (EPD) process in a magnetic field. Ceramics International, 2014, 40, 8369-8375.	4.8	11
138	Dynamic grain growth during low-temperature spark plasma sintering of alumina. Scripta Materialia, 2014, 80, 29-32.	5.2	36
139	Photoluminescent properties of new up-conversion phosphors of Yb/Tm co-doped (Gd1â^xLux)3Al5O12 (x=0.1–0.5) garnet solid solutions. Journal of Alloys and Compounds, 2014, 582, 623-627.	5.5	18
140	Synthesis of Highâ€Purity Ti ₃ SiC ₂ by Microwave Sintering. International Journal of Applied Ceramic Technology, 2014, 11, 911-918.	2.1	32
141	One-pot synthesis of monoclinic ZrO2 nanocrystals under subcritical hydrothermal conditions. Journal of Supercritical Fluids, 2014, 85, 57-61.	3.2	46
142	Reactive spark plasma sintering of binderless WC ceramics at 1500°C. International Journal of Refractory Metals and Hard Materials, 2014, 43, 42-45.	3.8	27
143	The effect of the interlayer element on the exfoliation of layered Mo ₂ AC (A = Al, Si, P, Ga,) Tj ETQq1 of Advanced Materials, 2014, 15, 014208.	1 0.78431 6.1	4 rgBT /Ove 78
144	Discovery of a new crystalline phase: BiGeO ₂ (OH) ₂ (NO ₃). CrystEngComm, 2014, 16, 10080-10088.	2.6	8

#	Article	IF	CITATIONS
145	Positional-dependent luminescence property of β-SiAlON:Eu2+ phosphor particle. Applied Physics Letters, 2014, 104, .	3.3	8
146	<i>In Situ</i> Fabrication of <scp><scp>B</scp></scp> Eutectic Composites by Spark–Plasma Sintering. Journal of the American Ceramic Society, 2014, 97, 2376-2378.	ub} 3.8	29
147	Controlled Photocatalytic Growth of Ag Nanocrystals on Brookite and Rutile and Their SERS Performance. ACS Applied Materials & Interfaces, 2014, 6, 236-243.	8.0	14
148	Densification behaviour and microstructural development in undoped yttria prepared by flash-sintering. Journal of the European Ceramic Society, 2014, 34, 991-1000.	5.7	159
149	Two-dimensional molybdenum carbides: potential thermoelectric materials of the MXene family. Physical Chemistry Chemical Physics, 2014, 16, 7841-7849.	2.8	395
150	Luminescent metal nanoclusters: controlled synthesis and functional applications. Science and Technology of Advanced Materials, 2014, 15, 014205.	6.1	63
151	Electric Doubleâ€Layer Capacitors Based on Highly Graphitized Nanoporous Carbons Derived from ZIFâ€67. Chemistry - A European Journal, 2014, 20, 7895-7900.	3.3	423
152	Systematic study on densification of alumina fine powder during milliwave sintering at 28ÂGHz. Journal of Asian Ceramic Societies, 2014, 2, 215-222.	2.3	6
153	Magnesium ion distribution and defect concentrations of MgO-doped lanthanum silicate oxyapatite. Solid State Ionics, 2014, 258, 24-29.	2.7	4
154	Direct Synthesis of MOFâ€Đerived Nanoporous Carbon with Magnetic Co Nanoparticles toward Efficient Water Treatment. Small, 2014, 10, 2096-2107.	10.0	588
155	Controlled Crystallization of Cyanoâ€Bridged Cu–Pt Coordination Polymers with Twoâ€Đimensional Morphology. Chemistry - an Asian Journal, 2014, 9, 1511-1514.	3.3	14
156	Pressureless Sintering and Reaction Mechanisms of <scp><scp>Ti</scp></scp> 3 <scp><scp>SiC</scp>2 Ceramics. Journal of the American Ceramic Society, 2014, 97, 1407-1412.</scp>	3.8	24
157	Fabrication of textured alumina by magnetic alignment via gelcasting based on low-toxic system. Journal of the European Ceramic Society, 2014, 34, 3841-3848.	5.7	19
158	Microstructure and adsorption property of nanocarbide-derived carbon (CDC) synthesized at ambient temperature. Materials Letters, 2014, 130, 188-191.	2.6	8
159	Toughness control of boron carbide obtained by spark plasma sintering in nitrogen atmosphere. Ceramics International, 2014, 40, 3053-3061.	4.8	34
160	Fabrication of Textured Ti3SiC2 Ceramics by Slip Casting in a Magnetic Field and Pulsed Electric Current Sintering. Journal of the Society of Powder Technology, Japan, 2014, 51, 163-168.	0.1	2
161	Tough and dense boron carbide obtained by high-pressure (300 MPa) and low-temperature (1600°C) spark plasma sintering. Journal of the Ceramic Society of Japan, 2014, 122, 271-275.	1.1	25
162	B ₆ O ceramic by <i>in-situ</i> reactive spark plasma sintering of a B ₂ O ₃ and B powder mixture. Journal of the Ceramic Society of Japan, 2014, 122, 336-340.	1.1	11

#	Article	IF	CITATIONS
163	Preparation of siloxane-containing vaterite doped with magnesium. Journal of the Ceramic Society of Japan, 2014, 122, 1010-1015.	1.1	7
164	Transparent ZnAl ₂ O ₄ ceramics fabricated by spark plasma sintering. Journal of the Ceramic Society of Japan, 2014, 122, 784-787.	1.1	23
165	Fabrication of textured Ti ₃ SiC ₂ ceramic by slip casting in a strong magnetic field and pressureless sintering. Journal of the Ceramic Society of Japan, 2014, 122, 817-821.	1.1	18
166	Low-Tepmerature Synthesis Process of Lanthanum Germanate Oxyapatite by Citrate Combustion Method. Funtai Oyobi Fummatsu Yakin/Journal of the Japan Society of Powder and Powder Metallurgy, 2014, 61, 582-586.	0.2	3
167	Influence of Loading Condition on Fabrication of Transparent MgAl ₂ O ₄ Spinel Ceramics by Spark-Plasma-Sintering (SPS) Technique. Funtai Oyobi Fummatsu Yakin/Journal of the Japan Society of Powder and Powder Metallurgy, 2014, 61, 565-574.	0.2	0
168	Metal-Ceramic/Ceramic Nanostructured Layered Composites for Solid Oxide Fuel Cells by Spark Plasma Sintering. Journal of Nanoscience and Nanotechnology, 2014, 14, 4218-4223.	0.9	3
169	Hybrid hydrogels containing vertically aligned carbon nanotubes with anisotropic electrical conductivity for muscle myofiber fabrication. Scientific Reports, 2014, 4, 4271.	3.3	213
170	TEM Characterization of Nanocomposite Materials. , 2014, , 333-373.		0
171	Fabrication of Textured Ceramics Using Mn and Nb-doped Hexagonal BaTiO ₃ by an Electrophoretic Deposition in a High Magnetic Field. Transactions of the Materials Research Society of Japan, 2014, 39, 199-202.	0.2	1
172	Theoretical modeling of electrode impedance for an oxygen ion conductor and metallic electrode system based on the interfacial conductivity theory. Solid State Ionics, 2013, 232, 49-57.	2.7	10
173	Spark plasma sintering of damage tolerant and machinable YAM ceramics. Journal of Advanced Ceramics, 2013, 2, 193-200.	17.4	3
174	Dielectrophoretically Aligned Carbon Nanotubes to Control Electrical and Mechanical Properties of Hydrogels to Fabricate Contractile Muscle Myofibers. Advanced Materials, 2013, 25, 4028-4034.	21.0	236
175	Transparent hydroxyapatite ceramics consolidated by spark plasma sintering. Scripta Materialia, 2013, 69, 366-369.	5.2	29
176	Structure characterization and photoluminescence properties of (Y0.95â^'xGdxEu0.05)2O3 red phosphors converted from layered rare-earth hydroxide (LRH) nanoflake precursors. Journal of Alloys and Compounds, 2013, 559, 188-195.	5.5	36
177	Mechanochemical activation of aluminum powder and synthesis of alumina based ceramic composites. Ceramics International, 2013, 39, 8141-8146.	4.8	8
178	Doped-carbon electrocatalysts with trimodal porosity from a homogeneous polypeptide gel. Journal of Materials Chemistry A, 2013, 1, 13576.	10.3	51
179	Grain-boundary sliding model of pore shrinkage in late intermediate sintering stage under hydrostatic pressure. Acta Materialia, 2013, 61, 6661-6669.	7.9	10
180	Greatly enhanced Dy3+ emission via efficient energy transfer in gadolinium aluminate garnet (Gd3Al5O12) stabilized with Lu3+. Journal of Materials Chemistry C, 2013, 1, 7614.	5.5	86

#	Article	IF	CITATIONS
181	Controlled Thermal Plasma Processing ofÂCeramic Nanopowders. , 2013, , 979-989.		0
182	Microstructure and mechanical properties of ZrB2–SiC–BN composites fabricated by reactive hot pressing and reactive spark plasma sintering. Scripta Materialia, 2013, 68, 889-892.	5.2	25
183	Machinable ZrB2–SiC–BN composites fabricated by reactive spark plasma sintering. Materials Science & Engineering A: Structural Materials: Properties, Microstructure and Processing, 2013, 582, 41-46.	5.6	39
184	Spark Plasma Sintered Ni-YSZ/YSZ Bi-Layers for Solid Oxide Fuel Cell. Journal of Nanoscience and Nanotechnology, 2013, 13, 4150-4157.	0.9	5
185	Transparent nanocrystalline bulk alumina obtained at 7.7GPa and 800°C. Scripta Materialia, 2013, 69, 362-365.	5.2	59
186	Preparation of Barium Titanate Grain-Oriented Ceramics by Electrophoresis Deposition Method under High Magnetic Field Using Single-Domain Nanoparticles. Key Engineering Materials, 2013, 582, 27-31.	0.4	2
187	Efficient green-luminescent germanium nanocrystals. Journal of Materials Chemistry A, 2013, 1, 3747.	10.3	30
188	Fabrication of the c-axis oriented zeolite L compacts using strong magnetic field. Materials Letters, 2013, 93, 408-410.	2.6	9
189	Theoretical modeling of electrode impedance for an oxygen ion conductor and metallic electrode system based on the interfacial conductivity theory. Part II: Case of the limiting process by non-steady-state surface diffusion. Solid State Ionics, 2013, 249-250, 78-85.	2.7	8
190	Effect of Gd2O3 on the thermal conductivity of ZrO2–4mol.% Y2O3 ceramics fabricated by spark plasma sintering. Scripta Materialia, 2013, 69, 165-170.	5.2	20
191	Synthesis, microstructure and mechanical properties of reactively sintered ZrB 2 –SiC–ZrN composites. Ceramics International, 2013, 39, 7273-7277.	4.8	14
192	Analysis of abnormal grain growth of oriented LiCoO2 prepared by slip casting in a strong magnetic field. Journal of the European Ceramic Society, 2013, 33, 3059-3064.	5.7	14
193	Development of Eu3+ activated monoclinic, perovskite, and garnet compounds in the Gd2O3–Al2O3 phase diagram as efficient red-emitting phosphors. Journal of Solid State Chemistry, 2013, 206, 104-112.	2.9	34
194	Nanocrystalline ZrB ₂ powders prepared by mechanical alloying. Journal of Asian Ceramic Societies, 2013, 1, 304-307.	2.3	15
195	Surface modification of Ca-α-SiAlON: Eu2+ phosphor particles by SiO2 coating and fabrication of its deposit by electrophoretic deposition (EPD) process. Applied Surface Science, 2013, 280, 229-234.	6.1	28
196	Size-Dependent Color Tuning of Efficiently Luminescent Germanium Nanoparticles. Langmuir, 2013, 29, 7401-7410.	3.5	66
197	NMR, ESR, and Luminescence Characterization of Bismuth Embedded Zeolites Y. Journal of Physical Chemistry C, 2013, 117, 6399-6408.	3.1	35
198	Perfect Highâ€Temperature Plasticity Realized in Multiwalled Carbon Nanotubeâ€Concentrated αâ€ <scp><scp>Al</scp></scp> ₂ <scp><scp>O</scp></scp> ₃ Hybrid. Journal of the American Ceramic Society, 2013, 96, 1904-1908.	3.8	14

#	Article	IF	CITATIONS
199	Highly transparent α-alumina obtained by low cost high pressure SPS. Ceramics International, 2013, 39, 3243-3248.	4.8	81
200	Novel Electronic and Magnetic Properties of Twoâ€Dimensional Transition Metal Carbides and Nitrides. Advanced Functional Materials, 2013, 23, 2185-2192.	14.9	1,418
201	Reactive spark plasma sintering of ZrC and HfC ceramics with fine microstructures. Scripta Materialia, 2013, 69, 139-142.	5.2	59
202	Layered rare-earth hydroxide and oxide nanoplates of the Y/Tb/Eu system: phase-controlled processing, structure characterization and color-tunable photoluminescence via selective excitation and efficient energy transfer. Science and Technology of Advanced Materials, 2013, 14, 015006.	6.1	50
203	Fabrication of Dense ZrO2/CNT Composites: Influence of Bead-Milling Treatment. Metallurgical and Materials Transactions A: Physical Metallurgy and Materials Science, 2013, 44, 4374-4381.	2.2	11
204	Unprecedented simultaneous enhancement in strain tolerance, toughness and strength of Al ₂ O ₃ ceramic by multiwall-type failure of a high loading of carbon nanotubes. Nanotechnology, 2013, 24, 155702.	2.6	37
205	Reaction temperature variations on the crystallographic state of spinel cobalt aluminate. Dalton Transactions, 2013, 42, 7167.	3.3	47
206	The development of Ce ³⁺ -activated (Gd,Lu) ₃ Al ₅ O ₁₂ garnet solid solutions as efficient yellow-emitting phosphors. Science and Technology of Advanced Materials, 2013, 14, 054201.	6.1	53
207	Controlled processing of (Gd,Ln) ₂ O ₃ :Eu (Ln = Y, Lu) red phosphor particles and compositional effects on photoluminescence. Science and Technology of Advanced Materials, 2013, 14, 064202.	6.1	30
208	Twoâ€Dimensional Orientation in <scp><scp>Bi</scp></scp> ₄ <scp><icp>Ti</icp></scp> ₃ <scp>O</scp> Prepared Using Platelet Particles and a Magnetic Field. Journal of the American Ceramic Society, 2013, 96, 1085-1089.	_{12< 3.8}	/sub≥ 15
209	Ideal design of textured LiCoO2 sintered electrode for Li-ion secondary battery. APL Materials, 2013, 1, .	5.1	20
210	Lowâ€Temperature Spark Plasma Sintering of Pure Nano <scp>WC</scp> Powder. Journal of the American Ceramic Society, 2013, 96, 1702-1705.	3.8	38
211	pH localization: a case study during electrophoretic deposition of ternary MAX phase carbide-Ti ₃ SiC ₂ . Journal of the Ceramic Society of Japan, 2013, 121, 348-354.	1.1	23
212	Electrophoretic deposition of orientation-controlled zeolite L layer on porous ceramic substrate. Journal of the Ceramic Society of Japan, 2013, 121, 370-372.	1.1	5
213	Damage and wear resistance of Al ₂ O ₃ –CNT nanocomposites fabricated by spark plasma sintering. Journal of the Ceramic Society of Japan, 2013, 121, 867-872.	1.1	7
214	High-temperature phase in zirconia film fabricated by aerosol gas deposition and its change upon subsequent heat treatment. Journal of the Ceramic Society of Japan, 2013, 121, 333-337.	1.1	4
215	Fabrication of textured Ti ₃ AlC ₂ by spark plasma sintering and their anisotropic mechanical properties. Journal of the Ceramic Society of Japan, 2013, 121, 366-369.	1.1	23
216	Electric field in SPS: geometry and pulsed current effects. Journal of the Ceramic Society of Japan, 2013, 121, 524-526.	1.1	16

#	Article	IF	CITATIONS
217	Hydrothermal transformation of magnetically orientation-controlled seed layer into orientation-retained dense, continuous film in clear reaction solution. Journal of the Ceramic Society of Japan, 2013, 121, 550-554.	1.1	1
218	Fabrication of textured α-alumina in high magnetic field via gelcasting with the use of glucose derivative. Journal of the Ceramic Society of Japan, 2013, 121, 89-94.	1.1	7
219	Synthesis of B ₆ O powder and spark plasma sintering of B ₆ O and B ₆ O–B ₄ C ceramics. Journal of the Ceramic Society of Japan, 2013, 121, 950-955.	1.1	35
220	Fabrication of Textured BaTiO ₃ Ceramics by Electrophoretic Deposition in A High Magnetic Field using Single-domain Particles. Transactions of the Materials Research Society of Japan, 2013, 38, 41-44.	0.2	4
221	Gadolinium Aluminate Garnet (<scp><scp>Gd₃Al₅O₁₂</scp></scp>): Crystal Structure Stabilization via Lutetium Doping and Properties of the (<scp><scp>Gd</scp></scp>	3.8 /sub> <scp< td=""><td>29 > < scp > Al <s< td=""></s<></td></scp<>	29 > < scp > Al <s< td=""></s<>
222	Orientation Control of Hematite via Transformation of Textured Goethite Prepared by EPD in a Strong Magnetic Field. Key Engineering Materials, 2012, 507, 227-231.	0.4	1
223	Tailoring Plate-Like Grained ZrB ₂ Ceramic via a Strong Magnetic Field Alignment Method Followed by Spark Plasma Sintering. Key Engineering Materials, 2012, 512-515, 702-705.	0.4	0
224	One-step route to a hybrid TiO2/TixW1â^'xN nanocomposite byin situselective carbothermal nitridation. Science and Technology of Advanced Materials, 2012, 13, 035001.	6.1	8
225	Effective lattice stabilization of gadolinium aluminate garnet (GdAG) via Lu ³⁺ doping and development of highly efficient (Gd,Lu)AG:Eu ³⁺ red phosphors. Science and Technology of Advanced Materials, 2012, 13, 035007.	6.1	43
226	Hydrogen generation from water using Mg nanopowder produced by arc plasma method. Science and Technology of Advanced Materials, 2012, 13, 025009.	6.1	36
227	Development of High-Strain-Rate Superplastic Oxide Ceramics Based on Flow Mechanism. Materials Science Forum, 2012, 735, 9-14.	0.3	2
228	Phase relationships in the quasi-ternary LaO1.5–SiO2–MgO system at 1773 K. Science and Technology of Advanced Materials, 2012, 13, 045006.	6.1	7
229	High Hardness B _{<i>a</i>} C _{<i>b</i>} -(B _{<i>x</i>} O _{<i>y</i>} /BN) Composites with 3D Mesh-Like Fine Grain-Boundary Structure by Reactive Spark Plasma Sintering. Journal of Nanoscience and Nanotechnology. 2012. 12, 959-965.	0.9	24
230	Textured Ti ₃ SiC ₂ by gelcasting in a strong magnetic field. Journal of the Ceramic Society of Japan, 2012, 120, 544-547.	1.1	11
231	White-light-emitting Liquefiable Silicon Nanocrystals. Chemistry Letters, 2012, 41, 1157-1159.	1.3	17
232	High-pressure spark plasma sintering of MgO-doped transparent alumina. Journal of the Ceramic Society of Japan, 2012, 120, 116-118.	1.1	48
233	Fabrication and Analysis of the Oriented <scp><scp>LiCoO</scp></scp> ₂ by Slip Casting in a Strong Magnetic Field. Journal of the American Ceramic Society, 2012, 95, 3428-3433.	3.8	11
234	Ultra-broad near-infrared photoluminescence from crystalline (K-crypt)2Bi2 containing [Bi2]2â^' dimers. Journal of Materials Chemistry, 2012, 22, 20175.	6.7	32

#	Article	lF	CITATIONS
235	Electrophoretic Deposition of <scp><scp>Ti</scp></scp> ₃ <scp>SiC</scp> 2 and Texture Development in a Strong Magnetic Field. Journal of the American Ceramic Society, 2012, 95, 2857-2862.	3.8	27
236	Influence of the zirconia transformation on the thermal behavior of zircon–zirconia composites. Journal of Thermal Analysis and Calorimetry, 2012, 110, 695-705.	3.6	14
237	Fluorescent and paramagnetic core–shell hybrid nanoparticles for bi-modal magnetic resonance/luminescence imaging. Journal of Materials Chemistry, 2012, 22, 20641.	6.7	24
238	Impact of magnetic field on molecular alignment and electrical conductivity in phthalocyanine nanowires. Journal of Materials Chemistry, 2012, 22, 8629.	6.7	18
239	Effect of Alumina Dopant on Transparency of Tetragonal Zirconia. Journal of Nanomaterials, 2012, 2012, 1-5.	2.7	41
240	Densification Kinetics of Nanocrystalline Zirconia Powder Using Microwave and Spark Plasma Sintering—A Comparative Study. Journal of Nanoscience and Nanotechnology, 2012, 12, 4577-4582.	0.9	14
241	Well-defined crystallites autoclaved from the nitrate/NH4OH reaction system as the precursor for (Y,Eu)2O3 red phosphor: Crystallization mechanism, phase and morphology control, and luminescent property. Journal of Solid State Chemistry, 2012, 192, 229-237.	2.9	39
242	Effective preparation of SiC nanoparticles by the reaction of thermal nitrogen plasma with solid SiC. Journal of Alloys and Compounds, 2012, 520, 127-131.	5.5	8
243	Peculiarities of the neck growth process during initial stage of spark-plasma, microwave and conventional sintering of WC spheres. Journal of Alloys and Compounds, 2012, 523, 1-10.	5.5	82
244	The effects of Gd3+ substitution on the crystal structure, site symmetry, and photoluminescence of Y/Eu layered rare-earth hydroxide (LRH) nanoplates. Dalton Transactions, 2012, 41, 1854-1861.	3.3	58
245	Electrical conductivity and X-ray diffraction analysis of oxyapatite-type lanthanum silicate and neodymium silicate solid solution. Solid State Ionics, 2012, 225, 443-447.	2.7	5
246	Synchrotron X-ray, Photoluminescence, and Quantum Chemistry Studies of Bismuth-Embedded Dehydrated Zeolite Y. Journal of the American Chemical Society, 2012, 134, 2918-2921.	13.7	64
247	Study of phase transformation behaviour of alumina through precipitation method. Journal Physics D: Applied Physics, 2012, 45, 215302.	2.8	29
248	Near-infrared photoluminescence from molecular crystals containing tellurium. Journal of Materials Chemistry, 2012, 22, 24792.	6.7	10
249	Photoluminescence from Bi5(GaCl4)3 molecular crystal. Dalton Transactions, 2012, 41, 11055.	3.3	29
250	Porous calcium sulfate ceramics with tunable degradation rate. Journal of Materials Science: Materials in Medicine, 2012, 23, 2437-2443.	3.6	17
251	Fabrication of Ceria- and Lanthanium Gallate-based Solid Electrolyte Layers on Porous NiO-YSZ by Sequential Electrophoretic Deposition Process. Funtai Oyobi Fummatsu Yakin/Journal of the Japan Society of Powder and Powder Metallurgy, 2012, 59, 626-630.	0.2	3
252	Highly Concentrated 3D Macrostructure of Individual Carbon Nanotubes in a Ceramic Environment. Advanced Materials, 2012, 24, 4322-4326.	21.0	56

#	Article	IF	CITATIONS
253	Experimental and theoretical studies of photoluminescence from Bi82+ and Bi53+ stabilized by [AlCl4]â°' in molecular crystals. Journal of Materials Chemistry, 2012, 22, 12837.	6.7	49
254	Synthesis of Plate‣ike <scp><scp>ZrB₂</scp> </scp> Grains. Journal of the American Ceramic Society, 2012, 95, 85-88.	3.8	30
255	Spark Plasma Sintering of Diamond Binderless <scp>WC</scp> Composites. Journal of the American Ceramic Society, 2012, 95, 2423-2428.	3.8	27
256	Strong <scp><scp>ZrB</scp></scp> ₂ – <scp><scp>SiC</scp>–<scp><scp>WC</scp></scp> Ceramics at 1600°C. Journal of the American Ceramic Society, 2012, 95, 874-878.</scp>	3.8	50
257	Dense zircon (ZrSiO4) ceramics by high energy ball milling and spark plasma sintering. Ceramics International, 2012, 38, 1793-1799.	4.8	55
258	Grain boundary diffusion driven spark plasma sintering of nanocrystalline zirconia. Ceramics International, 2012, 38, 4385-4389.	4.8	26
259	Orientation control of mordenite zeolite in strong magnetic field. Microporous and Mesoporous Materials, 2012, 151, 188-194.	4.4	16
260	Optical and adhesive properties of composite silica-impregnated Ca-α-SiAlON:Eu2+ phosphor films prepared on silica glass substrates. Journal of the European Ceramic Society, 2012, 32, 1365-1369.	5.7	7
261	Microstructure characterization of ZrB2–SiC composite fabricated by spark plasma sintering with TaSi2 additive. Journal of the European Ceramic Society, 2012, 32, 1441-1446.	5.7	32
262	Zircon–zirconia (ZrSiO4–ZrO2) dense ceramic composites by spark plasma sintering. Journal of the European Ceramic Society, 2012, 32, 787-793.	5.7	46
263	High-temperature bending strength, internal friction and stiffness of ZrB2–20vol% SiC ceramics. Journal of the European Ceramic Society, 2012, 32, 2519-2527.	5.7	112
264	Effect of loading schedule on densification of MgAl2O4 spinel during spark plasma sintering (SPS) processing. Journal of the European Ceramic Society, 2012, 32, 2303-2309.	5.7	37
265	EFFECT OF & beta;-CALCIUM ORTHOPHOSPHATE ADDITION ON HIGH- TEMPERATURE PLASTIC DEFORMATION OF HYDROXYAPATITE WITH SUBMICROMETER-SIZED GRAINS. Phosphorus Research Bulletin, 2012, 27, 11-17.	0.6	0
266	Fabrication of Highly-Densified Hydroxyapatite Ceramic with Boron Oxide Addition and Its Superplastic Deformation. IOP Conference Series: Materials Science and Engineering, 2011, 18, 022020.	0.6	2
267	Microstructure Control of Barium Titanate - Potassium Niobate Solid Solution System Ceramics by MPB Engineering and Their Piezoelectric Properties. IOP Conference Series: Materials Science and Engineering, 2011, 18, 092058.	0.6	0
268	Nanometer-thin layered hydroxide platelets of (Y0.95Eu0.05)2(OH)5NO3·xH2O: exfoliation-free synthesis, self-assembly, and the derivation of dense oriented oxide films of high transparency and greatly enhanced luminescence. Journal of Materials Chemistry, 2011, 21, 6903.	6.7	72
269	Hybrid dandelion-like YH(O3PC6H5)2:Ln (Ln = Eu3+, Tb3+) particles: formation mechanism, thermal and photoluminescence properties. CrystEngComm, 2011, 13, 5226.	2.6	6
270	Ultrabroad near-infrared photoluminescence from Bi5(AlCl4)3 crystal. Journal of Materials Chemistry, 2011, 21, 4060.	6.7	63

#	Article	IF	CITATIONS
271	Photoluminescence, cytotoxicity and in vitro imaging of hexagonal terbium phosphatenanoparticles doped with europium. Nanoscale, 2011, 3, 1263-1269.	5.6	56
272	Ultrabroad near-infrared photoluminescence from ionic liquids containing subvalent bismuth. Optics Letters, 2011, 36, 100.	3.3	51
273	Sensitized broadband near-infrared luminescence from bismuth-doped silicon-rich silica films. Optics Letters, 2011, 36, 4221.	3.3	16
274	Thermal conductivity of EB-PVD ZrO2–4mol% Y2O3 films using the laser flash method. Journal of Alloys and Compounds, 2011, 509, 1045-1049.	5.5	24
275	3rd International Congress on Ceramics (ICC3). IOP Conference Series: Materials Science and Engineering, 2011, 18, 001001.	0.6	6
276	Formation of Zirconia Films by the Aerosol Gas Deposition Method (By Jetting of Positive Charged) Tj ETQq0 0 0 2011, 58, 463-472.	rgBT /Ove 0.2	rlock 10 Tf 50 5
277	Application of new low toxic monomers in gelcasting process of alumina powder. IOP Conference Series: Materials Science and Engineering, 2011, 18, 072009.	0.6	2
278	Texture development in anatase and rutile prepared by slip casting in a strong magnetic field. Journal of the Ceramic Society of Japan, 2011, 119, 334-337.	1.1	13
279	Texture development of surface-modified SiC prepared by EPD in a strong magnetic field. Journal of the Ceramic Society of Japan, 2011, 119, 667-671.	1.1	4
280	Influence of La2O3 addition on thermophysical properties of ZrO2-4 mol %Y2O3 ceramics fabricated by spark plasma sintering. Journal of the Ceramic Society of Japan, 2011, 119, 929-932.	1.1	7
281	Modeling of the temperature distribution of flash sintered zirconia. Journal of the Ceramic Society of Japan, 2011, 119, 144-146.	1.1	111
282	Alignment of Carbon Nanofibers in the Al ₂ O ₃ Matrix under a Magnetic Field. Materials Transactions, 2011, 52, 572-575.	1.2	6
283	Appearance of high-temperature phase in zirconia films made by aerosol gas deposition method. Journal of the Ceramic Society of Japan, 2011, 119, 271-276.	1.1	21
284	Textured lead titanate ceramics fabricated by slip casting under a high magnetic field. Journal of the Ceramic Society of Japan, 2011, 119, 60-64.	1.1	8
285	Fabrication of the oriented LiCoO2 sheet using a strong magnetic field. Journal of the Ceramic Society of Japan, 2011, 119, 701-705.	1.1	8
286	Fabrication of Textured Nb ₄ AlC ₃ Ceramic by Slip Casting in a Strong Magnetic Field and Spark Plasma Sintering. Journal of the American Ceramic Society, 2011, 94, 410-415.	3.8	80
287	Tailoring Ti ₃ SiC ₂ Ceramic via a Strong Magnetic Field Alignment Method Followed by Spark Plasma Sintering. Journal of the American Ceramic Society, 2011, 94, 742-748.	3.8	57
288	Textured h-BN Ceramics Prepared by Slip Casting. Journal of the American Ceramic Society, 2011, 94, 1397-1404.	3.8	32

#	Article	IF	CITATIONS
289	Effects of Pressure Application Method on Transparency of Spark Plasma Sintered Alumina. Journal of the American Ceramic Society, 2011, 94, 1405-1409.	3.8	65
290	Phase Relation Studies in the ZrO2-CeO2-La2O3 System at 1500°C. Journal of the American Ceramic Society, 2011, 94, 1911-1919.	3.8	13
291	Highly Infrared Transparent Nanometric Tetragonal Zirconia Prepared by Highâ€Pressure Spark Plasma Sintering. Journal of the American Ceramic Society, 2011, 94, 2739-2741.	3.8	27
292	Fabrication of Transparent Yttria by Highâ€Pressure Spark Plasma Sintering. Journal of the American Ceramic Society, 2011, 94, 3206-3210.	3.8	66
293	Low-temperature formation of Ln silicate oxyapatite (Ln=La and Nd) by the water-based sol–gel method. Solid State Ionics, 2011, 204-205, 91-96.	2.7	12
294	Superplastic deformation of hydroxyapatite ceramics with B2O3 or Na2O addition fabricated by pulse current pressure sintering. Journal of the European Ceramic Society, 2011, 31, 2641-2648.	5.7	15
295	High-hardness B4C textured by a strong magnetic field technique. Scripta Materialia, 2011, 64, 256-259.	5.2	47
296	Shell-like nanolayered Nb4AlC3 ceramic with high strength and toughness. Scripta Materialia, 2011, 64, 765-768.	5.2	77
297	Effect of Bi(B)O3 perovskite substitution on enhanced tetragonality and ferroelectric transition temperature in Pb(Zr,Ti)O3 ceramics. Materials Chemistry and Physics, 2011, 129, 322-325.	4.0	11
298	Single-phased luminescent mesoporous nanoparticles for simultaneous cell imaging and anticancer drug delivery. Biomaterials, 2011, 32, 7226-7233.	11.4	68
299	Fabrication of dense β-calcium orthophosphate with submicrometer-sized grains and its high-temperature superplastic deformation. Journal of Materials Science, 2011, 46, 1956-1962.	3.7	1
300	Highly Fluorescent Silicaâ€Coated Bismuthâ€Doped Aluminosilicate Nanoparticles for Nearâ€Infrared Bioimaging. Small, 2011, 7, 199-203.	10.0	61
301	Colloidal processing of Gd2O3:Eu3+ red phosphor monospheres of tunable sizes: Solvent effects on precipitation kinetics and photoluminescence properties of the oxides. Acta Materialia, 2011, 59, 3688-3696.	7.9	69
302	†Beautiful' unconventional synthesis and processing technologies of superconductors and some other materials. Science and Technology of Advanced Materials, 2011, 12, 013001.	6.1	29
303	Monodisperse colloidal spheres for (Y,Eu)2O3red-emitting phosphors: establishment of processing window and size-dependent luminescence behavior. Science and Technology of Advanced Materials, 2011, 12, 055001.	6.1	24
304	Preparation and Characterization of Grain-Oriented Barium Titanate Ceramics Using Electrophoresis Deposition Method under a High Magnetic Field. Key Engineering Materials, 2011, 485, 313-316.	0.4	4
305	Preparation and Dielectric Properties of Dense Barium Titanate Nanoparticle Accumulations by Electrophoresis Deposition Method. Key Engineering Materials, 2011, 485, 35-38.	0.4	2
306	Physical and mechanical properties of highly textured polycrystalline Nb ₄ AlC ₃ ceramic. Science and Technology of Advanced Materials, 2011, 12, 044603.	6.1	50

ΥΟSΗΙΟ SAKKA

#	Article	IF	CITATIONS
307	Tough Yttria-Stabilized Zirconia Ceramic by Low-Temperature Spark Plasma Sintering of Long-Term Stored Nanopowders. Journal of Nanoscience and Nanotechnology, 2011, 11, 7901-7909.	0.9	5
308	Effect of sintering temperature on optical properties and microstructure of translucent zirconia prepared by high-pressure spark plasma sintering. Science and Technology of Advanced Materials, 2011, 12, 055003.	6.1	57
309	Microstructure Control of Barium Titanate – Potassium Niobate Solid Solution System Ceramics by MPB Engineering and their Piezoelectric Properties. Key Engineering Materials, 2011, 485, 89-92.	0.4	9
310	'Beautiful' unconventional synthesis and processing technologies of superconductors and some other materials. Science and Technology of Advanced Materials, 2011, 12, 013001.	6.1	3
311	Zirconia Nanoceramic via Redispersion of Highly Agglomerated Nanopowder and Spark Plasma Sintering. Journal of Nanoscience and Nanotechnology, 2010, 10, 6634-6640.	0.9	4
312	Emission color tuning of laminated and mixed SiAlON phosphor films by electrophoretic deposition. Journal of the Ceramic Society of Japan, 2010, 118, 1-4.	1.1	20
313	Influence of uni and bi-modal SiC composition on mechanical properties and microstructure of reaction-bonded SiC ceramics. Journal of the Ceramic Society of Japan, 2010, 118, 1028-1031.	1.1	10
314	Micro gas sensor assembly of tin oxide nano-particles by a capillary micro-molding process. Journal of the Ceramic Society of Japan, 2010, 118, 202-205.	1.1	5
315	Synthesis of SiC nano-powders from liquid carbon and various silica sources. Journal of the Ceramic Society of Japan, 2010, 118, 345-348.	1.1	7
316	Controlled organic/inorganic interface leading to the size-tunable luminescence from Si nanoparticles. Journal of the Ceramic Society of Japan, 2010, 118, 932-939.	1.1	7
317	Dispersion and Shortening of Multi-Walled Carbon Nanotubes by Size Modification. Materials Transactions, 2010, 51, 192-195.	1.2	8
318	Effect of grain size on electrical properties of scandia-stabilized zirconia. Journal of the Ceramic Society of Japan, 2010, 118, 1038-1043.	1.1	9
319	Formation of zirconia films by aerosol gas deposition method using zirconia powder produced by break-down method. Journal of the Ceramic Society of Japan, 2010, 118, 948-951.	1.1	22
320	Formation of zirconia films by the aerosol gas deposition method. Journal of the Ceramic Society of Japan, 2010, 118, 767-770.	1.1	26
321	Microstructure and properties of ZrB2-SiC and HfB2-SiC composites fabricated by spark plasma sintering (SPS) using TaSi2 as sintering aid. Journal of the Ceramic Society of Japan, 2010, 118, 997-1001.	1.1	31
322	Determination of Easy Magnetization Axis of Mordenite Zeolite. Chemistry Letters, 2010, 39, 347-349.	1.3	9
323	Effect of alumina addition on initial sintering of cubic ZrO2 (8YSZ). Ceramics International, 2010, 36, 879-885.	4.8	27
324	Material properties controlling photocurrent on TiO2 aggregates with plane orientation for dye-sensitized solar cells. Journal of Nanoparticle Research, 2010, 12, 2621-2628.	1.9	6

#	Article	IF	CITATIONS
325	Fabrication of c-axis oriented zinc oxide by electrophoretic deposition in a rotating magnetic field. Journal of the European Ceramic Society, 2010, 30, 1171-1175.	5.7	13
326	Experimental verification of pH localization mechanism of particle consolidation at the electrode/solution interface and its application to pulsed DC electrophoretic deposition (EPD). Journal of the European Ceramic Society, 2010, 30, 1187-1193.	5.7	70
327	Gelcasting of alumina with a new monomer synthesized from glucose. Journal of the European Ceramic Society, 2010, 30, 1795-1801.	5.7	44
328	Effect of sintering conditions on microstructure orientation in α-SiC prepared by slip casting in a strong magnetic field. Journal of the European Ceramic Society, 2010, 30, 2813-2817.	5.7	44
329	Effect of pH localization on microstructure evolution of deposits during aqueous electrophoretic deposition (EPD). Journal of the European Ceramic Society, 2010, 30, 2467-2473.	5.7	32
330	Microstructure and properties of ZrB2–SiC composites prepared by spark plasma sintering using TaSi2 as sintering additive. Journal of the European Ceramic Society, 2010, 30, 2625-2631.	5.7	43
331	Effect of different modification agents on hydrogen-generation by the reaction of Al with water. International Journal of Hydrogen Energy, 2010, 35, 9561-9568.	7.1	128
332	Sizeâ€Tunable UV‣uminescent Silicon Nanocrystals. Small, 2010, 6, 915-921.	10.0	81
333	Coexistence of A―and Bâ€Site Vacancy Compensation in Laâ€Doped Sr _{1â^'<i>x</i>} Ba <i>_x</i> TiO ₃ . Journal of the American Ceramic Society, 2010, 93, 2903-2908.	3.8	16
334	Highly Transparent Pure Alumina Fabricated by Highâ€Pressure Spark Plasma Sintering. Journal of the American Ceramic Society, 2010, 93, 2460-2462.	3.8	85
335	Role of Modification Agent Coverage in Hydrogen Generation by the Reaction of Al with Water. Journal of the American Ceramic Society, 2010, 93, 2534-2536.	3.8	13
336	Role of Particle Sizes in Hydrogen Generation by the Reaction of Al with Water. Journal of the American Ceramic Society, 2010, 93, 2998-3001.	3.8	25
337	Forming and Microstructure Control of Ceramics by Electrophoretic Deposition (EPD). KONA Powder and Particle Journal, 2010, 28, 74-90.	1.7	31
338	Electrophretic Deposition of LDC/LSGM/LDC Tri-layers on NiO-YSZ for Anode-supported SOFC. Transactions of the Materials Research Society of Japan, 2010, 35, 723-725.	0.2	2
339	Photoelectrochemical evaluation of anatase TiO ₂ polycrystalline aggregation layers with different crystalline orientations. Journal of Materials Research, 2010, 25, 63-68.	2.6	4
340	Orientation Dependence of Semiconductor Properties in Anatase TiO[sub 2] Polycrystalline Aggregates. Journal of the Electrochemical Society, 2010, 157, H65.	2.9	15
341	Hybrid processing and anisotropic sintering shrinkage in textured ZnO ceramics. Science and Technology of Advanced Materials, 2010, 11, 065006.	6.1	14
342	Potential use of only Yb ₂ O ₃ in producing dense Si ₃ N ₄ ceramics with high thermal conductivity by gas pressure sintering. Science and Technology of Advanced Materials, 2010, 11, 065001.	6.1	34

#	Article	IF	CITATIONS
343	An efficient and biocompatible fluorescence resonance energy transfer system based on lanthanide-doped nanoparticles. Nanotechnology, 2010, 21, 455703.	2.6	23
344	Fluorescent sensing of colloidal CePO ₄ :Tb nanorods for rapid, ultrasensitive and selective detection of vitamin C. Nanotechnology, 2010, 21, 365501.	2.6	53
345	Layered Rare-Earth Hydroxides (LRHs) of (Y _{1â[°] <i>x</i>} Eu _{<i>x</i>}) ₂ (OH) ₅ NO ₃ · <i>n(<i>x</i> = 0â^{°1}1): Structural Variations by Eu³⁺ Doping, Phase Conversion to Oxides, and the Correlation of Photoluminescence Behaviors. Chemistry of Materials. 2010. 22. 4204-4213.</i>	>H _{2 6.7}	0
346	Near-infrared photoluminescence and Raman characterization of bismuth-embedded sodalite nanocrystals. Optics Letters, 2010, 35, 1743.	3.3	17
347	Magnetic field-induced off-resonance third-order optical nonlinearity of iron oxide nanoparticles incorporated mesoporous silica thin films during heat treatment. Optics Express, 2010, 18, 2010.	3.4	8
348	Synthesis, microstructure and mechanical properties of (Zr,Ti)B2-(Zr,Ti)N composites prepared by spark plasma sintering. Journal of Alloys and Compounds, 2010, 494, 266-270.	5.5	23
349	Synthesis, Microstructure and Mechanical Properties of ZrB ₂ Ceramic Prepared by Mechanical Alloying and Spark Plasma Sintering. Key Engineering Materials, 2010, 434-435, 165-168.	0.4	1
350	Interfacial-related color tuning of colloidal Si nanocrystals. Green Chemistry, 2010, 12, 2139.	9.0	41
351	Spectroscopic characterization of bismuth embedded Y zeolites. Applied Physics Letters, 2010, 97, .	3.3	24
352	Significant third-order optical nonlinearity enhancement of gold nanoparticle incorporated mesoporous silica thin films by magnetic field thermal treatment. Journal of Materials Chemistry, 2010, 20, 8399.	6.7	14
353	Sedimentation classification treatment effect of starting powders in slip casting on magneto-orientation of mordenite zeolite. Transactions of the Materials Research Society of Japan, 2010, 35, 701-703.	0.2	2
354	Electrical conductivity of Gd-doped ceria with nano-sized grain. Transactions of the Materials Research Society of Japan, 2009, 34, 555-559.	0.2	2
355	Preparation of Highly Oriented Transparent (Sr,Ba)Nb2O6Ceramics and Their Ferroelectric Properties. Japanese Journal of Applied Physics, 2009, 48, 031405.	1.5	18
356	3-Dimensional Grain Orientation of RE-Ba-Cu-O Superconductors Using a Modulated Oval Magnetic Field. IEEE Transactions on Applied Superconductivity, 2009, 19, 2961-2964.	1.7	14
357	Control of lattice spacing in a triangular lattice of feeble magnetic particles formed by induced magnetic dipole interactions. Science and Technology of Advanced Materials, 2009, 10, 014608.	6.1	7
358	Focus on materials analysis and processing in magnetic fields. Science and Technology of Advanced Materials, 2009, 10, 010301.	6.1	1
359	Magnetic orientation and magnetic anisotropy in paramagnetic layered oxides containing rare-earth ions. Science and Technology of Advanced Materials, 2009, 10, 014604.	6.1	35
360	Photoanode characteristics of dye-sensitized solar cell containing TiO2 layers with different crystalline orientations. Journal of Materials Research, 2009, 24, 1417-1421.	2.6	8

#	Article	IF	CITATIONS
361	Formation of Crystalline-Oriented Titania Thin Films on ITO Glass Electrodes by EPD in a Strong Magnetic Field. Key Engineering Materials, 2009, 412, 143-148.	0.4	2
362	Simultaneous alignment and micropatterning of carbon nanotubes using modulated magnetic field. Science and Technology of Advanced Materials, 2009, 10, 014603.	6.1	18
363	Fabrication of Multi-Layered Thermoelectric Thick Films and their Thermoelectric Performance. Key Engineering Materials, 2009, 412, 291-296.	0.4	0
364	Highly textured ZrB2-based ultrahigh temperature ceramics via strong magnetic field alignment. Scripta Materialia, 2009, 60, 615-618.	5.2	84
365	Textured HfB2-based ultrahigh-temperature ceramics with anisotropic oxidation behavior. Scripta Materialia, 2009, 60, 913-916.	5.2	39
366	Densification and Cell Performance of Gadolinium-Doped Ceria (GDC) Electrolyte/NiO-GDC Anode Laminates. Journal of the American Ceramic Society, 2009, 92, S117-S121.	3.8	28
367	Hydrolysis and Dispersion Properties of Aqueous Y ₂ Si ₂ O ₇ Suspensions. Journal of the American Ceramic Society, 2009, 92, 54-61.	3.8	17
368	Preparation of Crystallineâ€Oriented Titania Photoelectrodes on ITO Glasses from a 2â€Propanol–2,4â€Pentanedione Solvent by Electrophoretic Deposition in a Strong Magnetic Field. Journal of the American Ceramic Society, 2009, 92, 984-989.	3.8	25
369	Pressure Effect on the Homogeneity of Spark Plasmaâ€Sintered Tungsten Carbide Powder. Journal of the American Ceramic Society, 2009, 92, 2418-2421.	3.8	36
370	Wet Processing and Lowâ€Temperature Pressureless Sintering of SiC Using a Novel Al ₃ BC ₃ Sintering Additive. Journal of the American Ceramic Society, 2009, 92, 2888-2893.	3.8	18
371	Application of constant current pulse to suppress bubble incorporation and control deposit morphology during aqueous electrophoretic deposition (EPD). Journal of the European Ceramic Society, 2009, 29, 1837-1845.	5.7	70
372	Effect of sintering additive on crystallographic orientation in AlN prepared by slip casting in a strong magnetic field. Journal of the European Ceramic Society, 2009, 29, 2627-2633.	5.7	33
373	Micro-emulsion synthesis of blue-luminescent silicon nanoparticles stabilized with alkoxy monolayers. Journal of Crystal Growth, 2009, 311, 634-637.	1.5	28
374	Microstructure and high-temperature strength of B4C–TiB2 composite prepared by a crucibleless zone melting method. Journal of Alloys and Compounds, 2009, 485, 677-681.	5.5	61
375	Low temperature thermal expansion, high temperature electrical conductivity, and mechanical properties of Nb4AlC3 ceramic synthesized by spark plasma sintering. Journal of Alloys and Compounds, 2009, 487, 675-681.	5.5	39
376	Simple preparation of silica and alumina with a hierarchical pore system via the dual-templating method. Science and Technology of Advanced Materials, 2009, 10, 025002.	6.1	17
377	Electric current activated/assisted sintering (<i>ECAS</i>): a review of patents 1906–2008. Science and Technology of Advanced Materials, 2009, 10, 053001.	6.1	357
378	Elucidation of Crystal-Chemical Determination Factor of Magnetic Anisotropy in HTSC. IEEE Transactions on Applied Superconductivity, 2009, 19, 2965-2969.	1.7	0

ΥΟSΗΙΟ SAKKA

#	Article	IF	CITATIONS
379	Facile patterning of assembled silica nanoparticles with a closely packed arrangement through guided growth. Journal of Materials Chemistry, 2009, 19, 1964.	6.7	16
380	Laser-derived one-pot synthesis of silicon nanocrystals terminated with organic monolayers. Chemical Communications, 2009, , 4684.	4.1	71
381	Texture development in 3mol% yttria-stabilized tetragonal zirconia. Materials Research Bulletin, 2009, 44, 1802-1805.	5.2	15
382	Effect of starting powders on the sintering of nanostructured ZrO2ceramics by colloidal processing. Science and Technology of Advanced Materials, 2009, 10, 025004.	6.1	30
383	Control of Texture in Diamagnetic Ceramics by Using a Strong Magnetic Field. Materia Japan, 2009, 48, 321-326.	0.1	0
384	Pressure Effects on Temperature Distribution during Spark Plasma Sintering with Graphite Sample. Materials Transactions, 2009, 50, 2111-2114.	1.2	45
385	Effect of bead-milling treatment on the dispersion of tetragonal zirconia nanopowder and improvements of two-step sintering. Journal of the Ceramic Society of Japan, 2009, 117, 470-474.	1.1	13
386	3rd International Workshop on Materials Analysis and Processing in Magnetic Fields (MAP3). Journal of Physics: Conference Series, 2009, 156, 011001.	0.4	0
387	Fabrication of Textured Hematite via Topotactic Transformation of Textured Goethite. Applied Physics Express, 2009, 2, 101601.	2.4	1
388	Fabrication of GDC/LSGM/GDC tri-layers on polypyrrole-coated NiO-YSZ by electrophoretic deposition for anode-supported SOFC. Journal of the Ceramic Society of Japan, 2009, 117, 1246-1248.	1.1	20
389	Aqueous Dispersions of Carbon Nanotubes Stabilized by Zirconium Acetate. Journal of Nanoscience and Nanotechnology, 2009, 9, 662-665.	0.9	7
390	Wavelength-Selectivity in Photochemical Reaction Between 1-Alcohol and Hydrogen-Terminated Silicon. Journal of Nanoscience and Nanotechnology, 2009, 9, 666-669.	0.9	10
391	Si ₃ N ₄ –TiN Nanocomposite by Nitration of TiSi ₂ and Consolidation by Hot Pressing and Spark Plasma Sintering. Journal of Nanoscience and Nanotechnology, 2009, 9, 6381-6389.	0.9	17
392	FABRICATION OF FLUORAPATITE CERAMIC MATERIAL WITH SUBMICROME -45- TER-SIZED GRAINS AND ITS HIGH-TEMPERATURE PLASTIC DEFORMATION. Phosphorus Research Bulletin, 2009, 23, 45-51.	0.6	0
393	Solution Synthesis of Luminescent Silicon Nanoparticles. Journal of the Japan Society of Colour Material, 2009, 82, 516-521.	0.1	0
394	Fluorescence detection and imaging of amino-functionalized organic monolayer. Thin Solid Films, 2008, 516, 2541-2546.	1.8	17
395	Liquid Manipulation Lithography to Fabricate a Multifunctional Microarray of Organosilanes on an Oxide Surface under Ambient Conditions. Advanced Functional Materials, 2008, 18, 3049-3055.	14.9	16
396	Exploration of a Standing Mesochannel System with Antimatter/Matter Atomic Probes. Advanced Materials, 2008, 20, 4728-4733.	21.0	16

ΥΟSΗΙΟ SAKKA

#	Article	IF	CITATIONS
397	Texturing behavior in sintered reaction-bonded silicon nitride via strong magnetic field alignment. Journal of the European Ceramic Society, 2008, 28, 929-934.	5.7	12
398	Nanoreactor engineering and SPS densification of multimetal oxide ceramic nanopowders. Journal of the European Ceramic Society, 2008, 28, 919-927.	5.7	17
399	Fabrication and some properties of textured alumina-related compounds by colloidal processing in high-magnetic field and sintering. Journal of the European Ceramic Society, 2008, 28, 935-942.	5.7	55
400	Texture development of hydroxyapatite ceramics by colloidal processing in a high magnetic field followed by sintering. Materials Science & Engineering A: Structural Materials: Properties, Microstructure and Processing, 2008, 475, 27-33.	5.6	27
401	CONTROL OF NANOSTRUCTURE OF MATERIALS. , 2008, , 177-265.		0
402	Highly Texturing β-Sialon Via Strong Magnetic Field Alignment. Journal of the American Ceramic Society, 2008, 91, 620-623.	3.8	15
403	Conductive Polymer Coating on Nonconductive Ceramic Substrates for Use in the Electrophoretic Deposition Process. Journal of the American Ceramic Society, 2008, 91, 1674-1677.	3.8	26
404	Corrosion of ZrB ₂ Powder During Wet Processing – Analysis and Control. Journal of the American Ceramic Society, 2008, 91, 1715-1717.	3.8	26
405	Phosphate Esters as Dispersants for the Cathodic Electrophoretic Deposition of Alumina Suspensions. Journal of the American Ceramic Society, 2008, 91, 1923-1926.	3.8	20
406	Bubbleâ€Free Aqueous Electrophoretic Deposition (EPD) by Pulseâ€Potential Application. Journal of the American Ceramic Society, 2008, 91, 3154-3159.	3.8	68
407	Hydrogenâ€Generation Materials for Portable Applications. Journal of the American Ceramic Society, 2008, 91, 3825-3834.	3.8	132
408	Influence of microstructure on the thermophysical properties of sintered SiC ceramics. Journal of Alloys and Compounds, 2008, 463, 493-497.	5.5	52
409	<i>In situ</i> observation of magnetic orientation process of feeble magnetic materials under high magnetic fields. Science and Technology of Advanced Materials, 2008, 9, 024211.	6.1	12
410	Texturing of Si ₃ N ₄ Ceramics via Strong Magnetic Field Alignment. Key Engineering Materials, 2008, 368-372, 871-874.	0.4	6
411	Electrophoretic deposition of Eu2+ doped CaALPHASiAlON phosphor particles for packaging of flat pseudo-white light emitting devices. Journal of the Ceramic Society of Japan, 2008, 116, 740-743.	1.1	13
412	Fabrication of Hierarchically Porous Spherical Particles by Assembling Mesoporous Silica Nanoparticles via Spray Drying. Journal of Nanoscience and Nanotechnology, 2008, 8, 3101-3105.	0.9	22
413	Textured silicon nitride: processing and anisotropic properties. Science and Technology of Advanced Materials, 2008, 9, 033001.	6.1	142
414	Effect of MgSiN2 addition on gas pressure sintering and thermal conductivity of silicon nitride with Y2O3. Journal of the Ceramic Society of Japan, 2008, 116, 706-711.	1.1	24

Υοςηίο δάκκα

#	Article	IF	CITATIONS
415	Spherical Mesoporous Silica Particles with Titanium Dioxide Nanoparticles by an Aerosol-assisted Coassembly. Chemistry Letters, 2008, 37, 72-73.	1.3	18
416	Effects of Initial Punch-Die Clearance in Spark Plasma Sintering Process. Materials Transactions, 2008, 49, 2899-2906.	1.2	12
417	Magnetically induced orientation of mesochannels inside porous anodic alumina membranes under ultra high magnetic field of 30 T: Confirmation by TEM. Journal of the Ceramic Society of Japan, 2008, 116, 1244-1248.	1.1	12
418	Preparation and Properties of Al ₂ O ₃ -Mullite-SiC Nano-Composite by Slip Casting in a High Magnetic Field and Reaction Sintering. Key Engineering Materials, 2007, 336-338, 1133-1136.	0.4	1
419	Microstructural examination in high-strain-rate superplastically deformed tetragonal ZrO2 dispersed with 30 vol% MgAl2O4 spinel. Journal of Materials Research, 2007, 22, 801-813.	2.6	5
420	Thermoelectric Properties and Magnetic Anisotropies of Magnetically Grain-Oriented Sr- or Bi-doped Ca3Co4O9 Thick Films. Materials Research Society Symposia Proceedings, 2007, 1044, 1.	0.1	0
421	Aqueous Processing of Textured Silicon Nitride Ceramics by Slip Casting in a Strong Magnetic Field. Materials Science Forum, 2007, 534-536, 1009-1012.	0.3	3
422	Improvement of Thermoelectric Properties of p- and n-types Oxide Thick Films Fabricated by Electrophoretic Deposition. Materials Research Society Symposia Proceedings, 2007, 1044, 1.	0.1	0
423	Hydrogen Storage Properties of Nb-Zr-Fe Alloys Disintegrated by Hydrogen Gas. Materials Science Forum, 2007, 534-536, 73-76.	0.3	0
424	Direct Shaping of Alumina Ceramics by Electrophoretic Deposition Using Conductive Polymer-Coated Ceramic Substrates. Advanced Materials Research, 2007, 29-30, 227-230.	0.3	2
425	Fabrication and Some Properties of Textured Ceramics by Colloidal Processing in High Magnetic Field. Key Engineering Materials, 2007, 352, 101-106.	0.4	3
426	Synthesis and Properties of Multimetal Oxide Nanopowders via Nano-Explosive Technique. Materials Science Forum, 2007, 534-536, 125-128.	0.3	1
427	Preparation and Some Properties of Ni-TiN and Ni-TiC Nanocomposite Particles by DC Arc-Plasma. Key Engineering Materials, 2007, 336-338, 2082-2085.	0.4	0
428	Effect of Milling Treatment on Texture Development of Hydroxyapatite Ceramics by Slip Casting in High Magnetic Field. Materials Transactions, 2007, 48, 2861-2866.	1.2	21
429	Fabrication of Textured α-SiC Using Colloidal Processing and a Strong Magnetic Field. Materials Transactions, 2007, 48, 2883-2887.	1.2	20
430	<l>In Situ</l> Microscopic Observations of Magnetic Field Effects on the Growth of Silver Dendrites. Materials Transactions, 2007, 48, 2888-2892.	1.2	4
431	Texturing CaALPHASialon Via Strong Magnetic Field Alignment. Journal of the Ceramic Society of Japan, 2007, 115, 701-705.	1.1	6
432	Large-Scale Patterning of TiO2 Nano Powders Using Micro Molds. Journal of the Ceramic Society of Japan, 2007, 115, 697-700.	1.1	7

Υοςηίο δάκκα

#	Article	IF	CITATIONS
433	Synthesis of Titania Thin Films by Cathodic Electrolytic Deposition. Journal of the Ceramic Society of Japan, 2007, 115, 818-820.	1.1	3
434	Flexible Polymer Colloidal rystal Lasers with a Lightâ€Emitting Planar Defect. Advanced Materials, 2007, 19, 2067-2072.	21.0	106
435	Relation between microstructure, properties and spark plasma sintering (SPS) parameters of pure ultrafine WC powder. Science and Technology of Advanced Materials, 2007, 8, 644-654.	6.1	73
436	High-strain-rate superplasticity in oxide ceramics. Science and Technology of Advanced Materials, 2007, 8, 578-587.	6.1	41
437	Nano Ceramics Center, National Institute for Materials Science. Science and Technology of Advanced Materials, 2007, 8, 571-577.	6.1	2
438	Processing and properties of sintered reaction-bonded silicon nitride with Y2O3–MgSiN2: Effects of Si powder and Li2O addition. Acta Materialia, 2007, 55, 5581-5591.	7.9	42
439	Effect of Polyethylenimine on Hydrolysis and Dispersion Properties of Aqueous Si3N4Suspensions. Journal of the American Ceramic Society, 2007, 90, 797-804.	3.8	46
440	Layer Structure of Textured CaBi4Ti4O15Ceramics Fabricated by Slip Casting in High Magnetic Field. Journal of the American Ceramic Society, 2007, 90, 1463-1466.	3.8	18
441	Dispersion Behavior of ZrB2Powder in Aqueous Solution. Journal of the American Ceramic Society, 2007, 90, 3455-3459.	3.8	45
442	Improvement of thermoelectric performance in magnetically c-axis-oriented bismuth-based cobaltites. Scripta Materialia, 2007, 57, 333-336.	5.2	7
443	Magnetically Induced Orientation of Mesochannels in Mesoporous Silica Films at 30â€Tesla. Chemistry - an Asian Journal, 2007, 2, 1505-1512.	3.3	56
444	Thermophysical properties of porous SiC ceramics fabricated by pressureless sintering. Science and Technology of Advanced Materials, 2007, 8, 655-659.	6.1	70
445	Nano-explosion synthesis of multi-component ceramic nano-composites. Journal of the European Ceramic Society, 2007, 27, 585-592.	5.7	8
446	Magnetically induced orientation of mesochannels in 2D-hexagonal mesoporous silica films. Journal of Materials Chemistry, 2006, 16, 3693.	6.7	61
447	The Effect of Embedding Conditions on the Thermal Conductivity of .BETASi3N4. Journal of the Ceramic Society of Japan, 2006, 114, 1093-1096.	1.3	15
448	Electrophoretic Deposition of Alumina on Conductive Polymer-Coated Ceramic Substrates. Journal of the Ceramic Society of Japan, 2006, 114, 55-58.	1.3	19
449	Texture Development in Si3N4 Ceramics by Magnetic Field Alignment during Slip Casting. Journal of the Ceramic Society of Japan, 2006, 114, 979-987.	1.3	40
450	Multiple Nano-Blast Synthesis of PT/8Y-ZP Composite Nanopowders. Journal of Nanoscience and Nanotechnology, 2006, 6, 1625-1631.	0.9	3

#	Article	IF	CITATIONS
451	Circularly Polarized Laser Emission Induced by Supramolecular Chirality in Cholesteric Liquid Crystals. Journal of Nanoscience and Nanotechnology, 2006, 6, 1819-1822.	0.9	33
452	One-Dimensional Self-Assembly of Alkoxy-Capped Silicon Nanoparticles. Journal of Nanoscience and Nanotechnology, 2006, 6, 1823-1825.	0.9	7
453	Fabrication of Highly Microstructure Controlled Ceramics by Novel Colloidal Processing. Journal of the Ceramic Society of Japan, 2006, 114, 371-376.	1.3	23
454	Texture Development in Alumina Composites by Slip Casting in a Strong Magnetic Field. Journal of the Ceramic Society of Japan, 2006, 114, 59-62.	1.3	22
455	Micro-Scale Patterning of Ceramic Colloidal Suspension by Micro Molding in Capillaries (MIMIC) with Assistance of Highly Infiltrating Liquid. Journal of the Ceramic Society of Japan, 2006, 114, 725-728.	1.3	9
456	ã,»ãf©ãfŸãffã,¯æœ–™ã«ãĚã'ã,‹é«~速è¶å¡'性. Materia Japan, 2006, 45, 640-643.	0.1	0
457	Nano-Blast Synthesis of Nano-size CeO2-Gd2O3 Powders. Journal of the American Ceramic Society, 2006, 89, 1822-1826.	3.8	21
458	Effect of polyethylenimine on the dispersion and electrophoretic deposition of nano-sized titania aqueous suspensions. Journal of the European Ceramic Society, 2006, 26, 1555-1560.	5.7	124
459	Mechanical properties of textured, multilayered alumina produced using electrophoretic deposition in a strong magnetic field. Journal of the European Ceramic Society, 2006, 26, 661-665.	5.7	30
460	Control of texture in alumina by colloidal processing in a strong magnetic field. Science and Technology of Advanced Materials, 2006, 7, 356-364.	6.1	106
461	Surface design of monolayer-template for reproducible microfabrication of metal oxide film. Thin Solid Films, 2006, 499, 293-298.	1.8	6
462	An efficient matrix that resists the nonspecific adsorption of protein to fabricate carbohydrate arrays on silicon. Thin Solid Films, 2006, 499, 213-218.	1.8	9
463	Control of crystalline texture in polycrystalline TiO2 (Anatase) by electrophoretic deposition in a strong magnetic field. Journal of the European Ceramic Society, 2006, 26, 559-563.	5.7	49
464	A practical technique for the fabrication of highly ordered macroporous structures of inorganic oxides. Materials Research Bulletin, 2006, 41, 268-273.	5.2	19
465	Chiroptical Properties Induced in Chiral Photonic-Bandgap Liquid Crystals Leading to a Highly Efficient Laser-Feedback Effect. Advanced Materials, 2006, 18, 775-780.	21.0	76
466	Microstructural Design for Attaining High-Strain-Rate Superplasticity in Oxide Materials. Advances in Science and Technology, 2006, 45, 923.	0.2	1
467	High-Toughness Tetragonal Zirconia/Alumina Nano-Ceramics. Key Engineering Materials, 2006, 317-318, 615-618.	0.4	1
468	Mechanical Properties of Textured Alumina Prepared by Colloidal Processing in a Strong Magnetic Field. Materials Research Society Symposia Proceedings, 2006, 977, 1.	0.1	0

#	Article	IF	CITATIONS
469	Fabrication of multilayered oxide thermoelectric modules by electrophoretic deposition under high magnetic fields. Applied Physics Letters, 2006, 89, 081912.	3.3	30
470	Highly controlled orientation of CaBi4Ti4O15 using a strong magnetic field. Applied Physics Letters, 2006, 89, 132902.	3.3	20
471	Control of the Texture in Feeble Magnetic Ceramics Using Colloidal Processing in a Strong Magnetic Field. Funtai Oyobi Fummatsu Yakin/Journal of the Japan Society of Powder and Powder Metallurgy, 2006, 53, 479-487.	0.2	1
472	CONTROL OF PARTICLE ORIENTATION OF HYDROXYAPATITE UNDER A HIGH MAGNETIC FIELD. Phosphorus Research Bulletin, 2005, 19, 256-261.	0.6	0
473	Textured Development of Feeble Magnetic Ceramics by Colloidal Processing Under High Magnetic Field. Journal of the Ceramic Society of Japan, 2005, 113, 26-36.	1.3	223
474	Dispersion of SiC Suspensions with Cationic Dispersant of Polyethylenimine. Journal of the Ceramic Society of Japan, 2005, 113, 584-587.	1.3	15
475	Fracture Toughness of Yttria-Stabilized Cubic Zirconia (8Y-CSZ) Doped with Pure Silica. Nippon Kinzoku Gakkaishi/Journal of the Japan Institute of Metals, 2005, 69, 928-932.	0.4	0
476	Synthesis and Characterization of Nanosize Ceria-Gadolinia Powders. Journal of the Ceramic Society of Japan, 2005, 113, 101-106.	1.3	10
477	Microstructural Design for High-Strain-Rate Superplastic Oxide Ceramics. Journal of the Ceramic Society of Japan, 2005, 113, 191-197.	1.3	20
478	Densification and Superplasticity of Hydroxyapatite Ceramics. Journal of the Ceramic Society of Japan, 2005, 113, 669-673.	1.3	26
479	Preparation and proton conductivity of monodisperse nanocrystals of pyrochlore-type antimonic acid and its niobium-substituted materials. Electrochimica Acta, 2005, 50, 3205-3209.	5.2	6
480	Electrophoretic deposition of lead zirconate titanate (PZT) powder from ethanol suspension prepared with phosphate ester. Science and Technology of Advanced Materials, 2005, 6, 927-932.	6.1	37
481	Sonochemical Preparation and Properties of Pt-3Y-TZP Nano-Composites. Journal of the American Ceramic Society, 2005, 88, 639-644.	3.8	20
482	Modification of Al Particle Surfaces by gamma-Al2O3 and Its Effect on the Corrosion Behavior of Al. Journal of the American Ceramic Society, 2005, 88, 977-979.	3.8	78
483	Preparation of oriented bulk 5wt% Y2O3–AlN ceramics by slip casting in a high magnetic field and sintering. Scripta Materialia, 2005, 52, 583-586.	5.2	65
484	Fabrication of porous ceramics with controlled pore size by colloidal processing. Science and Technology of Advanced Materials, 2005, 6, 915-920.	6.1	49
485	Texture of Alumina by Neutron Diffraction and SEM-EBSD. Materials Science Forum, 2005, 495-497, 1395-1400.	0.3	12
486	Porous Al2O3/Al catalyst supports fabricated by an Al(OH)3/Al mixture and the effect of agglomerates. Journal of Materials Research, 2005, 20, 672-679.	2.6	4

#	Article	IF	CITATIONS
487	High Strain-Rate Superplastic Flow in ZrO ₂ -30vol% Spinel Composite. Materials Science Forum, 2005, 475-479, 2977-2980.	0.3	4
488	Fabrication of Grain-Aligned Bulks and Thick Films of Misfit Layered Cobalt Oxides by a Magneto-Scientific Process. Materials Research Society Symposia Proceedings, 2005, 886, 1.	0.1	1
489	Development of Thermoelectric Bi-Based Cobaltites with an Easy Axis of Magnetization Parallel to the C-Axis for Magnetic Alignment. Japanese Journal of Applied Physics, 2005, 44, L1263-L1266.	1.5	13
490	Area-selective assembly of high crystalline tin-doped–indium–oxide particles onto monolayer template. Journal of Vacuum Science and Technology A: Vacuum, Surfaces and Films, 2005, 23, 1146-1151.	2.1	8
491	Assembly of hydrothermally synthesized tin oxide nanocrystals. Journal of Vacuum Science and Technology A: Vacuum, Surfaces and Films, 2005, 23, 731-736.	2.1	3
492	Orientation of mesochannels in continuous mesoporous silica films by a high magnetic field. Journal of Materials Chemistry, 2005, 15, 1137.	6.7	99
493	Rietveld Texture Analysis of Alumina Ceramics by Neutron Diffraction. Chemistry of Materials, 2005, 17, 102-106.	6.7	22
494	Nanoexplosion Synthesis of Multimetal Oxide Ceramic Nanopowders. Nano Letters, 2005, 5, 2598-2604.	9.1	30
495	New Processing of Textured Ceramics by Colloidal Processing Under High Magnetic Field. Key Engineering Materials, 2005, 280-283, 721-728.	0.4	5
496	The Crystal Orientation Taking Account of Gravity Force under High Magnetic Field. ISIJ International, 2005, 45, 997-1000.	1.4	13
497	Effect of MgAl2O4 Spinel Dispersion on High-Strain-Rate Superplasticity in Tetragonal ZrO2 Polycrystal. Nippon Kinzoku Gakkaishi/Journal of the Japan Institute of Metals, 2005, 69, 356-361.	0.4	Ο
498	Role of Deformable Fine Spinel Particles in High-Strain-Rate Superplastic Flow of Tetragonal ZrO2. Materials Research Society Symposia Proceedings, 2004, 821, 288.	0.1	0
499	High-Toughness Tetragonal Zirconia and Zirconia/Alumina Nano-Ceramics. Key Engineering Materials, 2004, 264-268, 2347-2350.	0.4	1
500	High-Strain Rate Superplastic Zirconia Systems. Key Engineering Materials, 2004, 264-268, 285-288.	0.4	0
501	High-Strain-Rate Superplasticity in 3mol%-Y ₂ O ₃ -Stabilized Tetragonal ZrO ₂ Dispersed with 30vol% MgAl ₂ O ₄ Spinel. Materials Science Forum, 2004, 447-448, 329-334	0.3	6
502	Control of Texture in Al ₂ O ₃ Composites by Slip Casting in a Strong Magnetic Field Followed by Heating. Key Engineering Materials, 2004, 264-268, 245-248.	0.4	2
503	Strain Softening and Hardening during Superplasticâ€Like Flow in a Fineâ€Grained MgAl ₂ O ₄ Spinel Polycrystal. Journal of the American Ceramic Society, 2004, 87, 1102-1109.	3.8	15
504	Alignment of TiO2 particles by electrophoretic deposition in a high magnetic field. Materials Research Bulletin, 2004, 39, 2155-2161.	5.2	17

#	Article	IF	CITATIONS
505	Nano-engineering of zirconia–noble metals composites. Journal of the European Ceramic Society, 2004, 24, 469-473.	5.7	26
506	Fabrication of high-strain rate superplastic yttria-doped zirconia polycrystals by adding manganese and aluminum oxides. Journal of the European Ceramic Society, 2004, 24, 449-453.	5.7	38
507	Low-temperature preparation of lithium vanadium oxides by solution processing. Journal of the European Ceramic Society, 2004, 24, 405-408.	5.7	14
508	Preparation of porous materials with controlled pore size and porosity. Journal of the European Ceramic Society, 2004, 24, 341-344.	5.7	137
509	Electrophoretic deposition of alumina suspension in a strong magnetic field. Journal of the European Ceramic Society, 2004, 24, 225-229.	5.7	55
510	Fabrication of oriented ?-alumina from porous bodies by slip casting in a high magnetic field. Solid State Ionics, 2004, 172, 341-347.	2.7	32
511	Bone-like Layer Growth and Adhesion of Osteoblast-like Cells on Calcium-deficient Hydroxyapatite Synthesized at Different pH. Materials Transactions, 2004, 45, 1782-1787.	1.2	6
512	Effect of MgAl ₂ O ₄ Spinel Dispersion on High-Strain-Rate Superplasticity in Tetragonal ZrO ₂ Polycrystal. Materials Transactions, 2004, 45, 2073-2077.	1.2	11
513	Fracture Toughness of Yttria-Stabilized Cubic Zirconia (8Y-CSZ) Doped with Pure Silica. Materials Transactions, 2004, 45, 3324-3329.	1.2	7
514	Preparation of macroporous titania from nanoparticle building blocks and polymer templates. Scripta Materialia, 2003, 49, 735-740.	5.2	15
515	Electrophoretic deposition of aqueous nano-sized zinc oxide suspensions on a zinc electrode. Materials Research Bulletin, 2003, 38, 207-212.	5.2	46
516	Preparation and Some Electrical Properties of Yttrium-Doped Antimonic Acids ChemInform, 2003, 34, no.	0.0	0
517	Preparation and lithium insertion property of layered LixV2O5·nH2O. Journal of Power Sources, 2003, 119-121, 201-204.	7.8	4
518	Lowâ€Temperature Processing and Mechanical Properties of Zirconia and Zirconia–Alumina Nanoceramics. Journal of the American Ceramic Society, 2003, 86, 299-304.	3.8	116
519	Role of the Initial Degree of Ionization of Polyethylenimine in the Dispersion of Silicon Carbide Nanoparticles. Journal of the American Ceramic Society, 2003, 86, 189-191.	3.8	64
520	Fabrication of Macroporous Alumina with Tailored Porosity. Journal of the American Ceramic Society, 2003, 86, 2050-2054.	3.8	89
521	Preparation and Some Electrical Properties of Yttrium-Doped Antimonic Acids. Chemistry of Materials, 2003, 15, 928-934.	6.7	23
522	Control of Texture in Electroceramics by Slip-Casting in a High Magnetic Field. Key Engineering Materials, 2003, 248, 191-194.	0.4	9

#	Article	IF	CITATIONS
523	Control of Crystal Orientation of Hydroxyapatite by using a High Magnetic Field. Key Engineering Materials, 2003, 240-242, 513-516.	0.4	15
524	Electrophoretic deposition of $\hat{l}\pm$ -alumina particles in a strong magnetic field. Journal of Materials Research, 2003, 18, 254-256.	2.6	29
525	Hardness and Fracture Toughness of Alumina-Doped Tetragonal Zirconia with Different Yttria Contents. Materials Transactions, 2003, 44, 2235-2238.	1.2	39
526	Control of Crystal Orientation of Hydroxyapatite by Imposition of a High Magnetic Field. Materials Transactions, 2003, 44, 1133-1137.	1.2	111
527	Fabrication of Ordered Macroporous Structures Based on Hetero-Coagulation Process Using Nanoparticle as Building Blocks. Chemistry Letters, 2003, 32, 276-277.	1.3	12
528	Alignment of Titania Whisker by Colloidal Filtration in a High Magnetic Field. Japanese Journal of Applied Physics, 2002, 41, L1416-L1418.	1.5	58
529	Fabrication of Textured Titania by Slip Casting in a High Magnetic Field Followed by Heating. Japanese Journal of Applied Physics, 2002, 41, L1272-L1274.	1.5	75
530	Fabrication of Tailored Alumina-Based Ceramics Through Colloidal Processing. Key Engineering Materials, 2002, 224-226, 619-622.	0.4	3
531	Stabilization of Yttria Aqueous Suspension with Polyethylenimine and Electrophoretic Deposition Journal of the Ceramic Society of Japan, 2002, 110, 840-843.	1.3	21
532	Microstructure and Superplasticity in Various Zirconia-Dispersed Aluminas Journal of the Ceramic Society of Japan, 2002, 110, 927-930.	1.3	1
533	Electrical Conductivity of a 3Y-TZP/Alumina Laminate Composite Synthesized by Electrophoretic Deposition Journal of the Ceramic Society of Japan, 2002, 110, 959-962.	1.3	6
534	Control of Texture in ZnO by Slip Casting in a Strong Magnetic Field and Heating. Chemistry Letters, 2002, 31, 1204-1205.	1.3	65
535	Electrophoretic deposition of aqueous nano-Î ³ -Al2O3 suspensions. Materials Research Bulletin, 2002, 37, 653-660.	5.2	55
536	Electrophoretic Deposition Behavior of Aqueous Nanosized Zinc Oxide Suspensions. Journal of the American Ceramic Society, 2002, 85, 2161-2165.	3.8	74
537	Highâ€Strainâ€Rate Superplasticity in Y ₂ O ₃ â€Stabilized Tetragonal ZrO ₂ Dispersed with 30 vol% MgAl ₂ O ₄ Spinel. Journal of the American Ceramic Society, 2002, 85, 1900-1902.	3.8	36
538	Processingâ€Dependent Microstructural Factors Affecting Cavitation Damage and Tensile Ductility in a Superplastic Alumina Dispersed with Zirconia. Journal of the American Ceramic Society, 2002, 85, 2763-2770.	3.8	25
539	Synthesis and Sintering of Zirconia Nano-Powder by Non-Isothermal Decomposition from Hydroxide Journal of the Ceramic Society of Japan, 2001, 109, 500-505.	1.3	17
540	Preferred Orientation of the Texture in the SiC Whisker-Dispersed Al2O3 Ceramics by Slip Casting in a High Magnetic Field Journal of the Ceramic Society of Japan, 2001, 109, 886-890.	1.3	40

Υοςηίο δάκκα

#	Article	IF	CITATIONS
541	Sintering and Ionic Conductivity of CuO-Doped Tetragonal ZrO2 Prepared by Novel Colloidal Processing Journal of the Ceramic Society of Japan, 2001, 109, 1004-1009.	1.3	6
542	Superplasticity in alumina enhanced by co-dispersion of 10% zirconia and 10% spinel particles. Acta Materialia, 2001, 49, 887-895.	7.9	48
543	A high-strain-rate superplastic ceramic. Nature, 2001, 413, 288-291.	27.8	245
544	Influence of Washing on Zirconia Powder for Electrophoretic Deposition. Journal of the American Ceramic Society, 2001, 84, 666-668.	3.8	20
545	Nonisothermal Synthesis of Yttriaâ€Stabilized Zirconia Nanopowder through Oxalate Processing: II, Morphology Manipulation. Journal of the American Ceramic Society, 2001, 84, 2484-2488.	3.8	31
546	Synthesis and Colloidal Processing of Zirconia Nanopowder. Journal of the American Ceramic Society, 2001, 84, 2489-2494.	3.8	156
547	Hydroxide synthesis, colloidal processing and sintering of nano-size 3Y-TZP powder. Scripta Materialia, 2001, 44, 2219-2223.	5.2	34
548	Effect of cavitation on superplastic flow of 10% zirconia-dispersed alumina. Scripta Materialia, 2001, 45, 61-67.	5.2	8
549	High Temperature Deformation of a Yttria-Stabilized Tetragonal Zirconia. Materials Science Forum, 2001, 357-359, 187-192.	0.3	3
550	Fabrication of Textured Alumina through Slip Casting in a High Magnetic Field and Heating. Key Engineering Materials, 2001, 206-213, 349-352.	0.4	3
551	Dense, bubble-free ceramic deposits from aqueous suspensions by electrophoretic deposition. Journal of Materials Research, 2001, 16, 321-324.	2.6	91
552	Colloidal Processing and Ionic Conductivity of Fineâ€Grained Cupricâ€Oxideâ€Doped Tetragonal Zirconia. Journal of the American Ceramic Society, 2001, 84, 2129-2131.	3.8	6
553	Effect of Ultrasonication on the Microstructure and Tensile Elongation of Zirconiaâ€Dispersed Alumina Ceramics Prepared by Colloidal Processing. Journal of the American Ceramic Society, 2001, 84, 2132-2134.	3.8	67
554	Synthesis of Aligned Alumina by Slip Casting in a High Magnetic Field and Heat Treatment Funtai Oyobi Fummatsu Yakin/Journal of the Japan Society of Powder and Powder Metallurgy, 2000, 47, 1010-1014.	0.2	17
555	Preparation, Electrical Properties, and Water Adsorption Behavior of (1-x)Sb2O5·xM2O3·nH2O (M = Al,) Tj ET	Qq]] 0.7	84314 rgBT
556	Enhanced superplasticity in a alumina-containing zirconia prepared by colloidal processing. Scripta Materialia, 2000, 43, 705-710.	5.2	47
557	Preparation of Polycrystalline Antimonic Acid Films by Electrophoretic Deposition. Journal of Sol-Gel Science and Technology, 2000, 19, 595-598.	2.4	4
558	The manufacturing process of fine Shirasu balloons using a fluidized sand-bed furnace. Advanced Powder Technology, 2000, 11, 503-516.	4.1	10

#	Article	IF	CITATIONS
559	Nonisothermal Synthesis of Yttria‣tabilized Zirconia Nanopowder through Oxalate Processing: I, Characteristics of Yâ€Zr Oxalate Synthesis and Its Decomposition. Journal of the American Ceramic Society, 2000, 83, 2196-2202.	3.8	47
560	Cavity Damage Accumulation in Alumina Doped with Zirconia or Magnesia. Materials Science Forum, 1999, 304-306, 431-436.	0.3	8
561	Superplastic Tensile Ductility in a Zirconia-Dispersed Alumina Produced by Colloidal Processing. Materials Science Forum, 1999, 304-306, 489-494.	0.3	3
562	A grain-boundary diffusion model of dynamic grain growth during superplastic deformation. Acta Materialia, 1999, 47, 3433-3439.	7.9	59
563	Preparation Methods and Superplastic Properties of Fine-Grained Zirconia and Alumina Based Ceramics Nippon Kagaku Kaishi / Chemical Society of Japan - Chemistry and Industrial Chemistry Journal, 1999, 1999, 497-508.	0.1	33
564	Effect of Ultrasonication on Colloidal Dispersion of Al ₂ O ₃ and ZrO ₂ Powders in pH Controlled Suspension. Materials Transactions, JIM, 1998, 39, 689-692.	0.9	25
565	Preparation and Properties of Lightweight Pottery Using Shirasuballoon. Journal of the Ceramic Society of Japan, 1998, 106, 333-338.	1.3	8
566	Colloidal Processing for Fine Particles of Al2O3-15vol% ZrO2 System Funtai Oyobi Fummatsu Yakin/Journal of the Japan Society of Powder and Powder Metallurgy, 1997, 44, 356-361.	0.2	12
567	Properties of Fine Shirasuballoons. Journal of the Ceramic Society of Japan, 1997, 105, 79-84.	1.3	7
568	Hydrogen sorption-desorption characteristics of mixed and composite Niî—,TiN nanoparticles. Scripta Materialia, 1996, 7, 341-353.	0.5	14
569	Preparation and Characterization of Fine Shirasuballoons. Journal of the Ceramic Society of Japan, 1996, 104, 963-968.	1.3	14
570	Hydrogen desorption characteristics of composite Co-TiN nanoparticles. Applied Surface Science, 1996, 100-101, 232-237.	6.1	13
571	Pressure Filtration of Al2O3 Small Powder Funtai Oyobi Fummatsu Yakin/Journal of the Japan Society of Powder and Powder Metallurgy, 1995, 42, 309-313.	0.2	4
572	Electro-discharge Sintering of (Fe,Co)-B and Ni-B Amorphous Ultrafine Powders Prepared by Chemical Reduction Funtai Oyobi Fummatsu Yakin/Journal of the Japan Society of Powder and Powder Metallurgy, 1995, 42, 323-329.	0.2	1
573	Processing of Silicon Carbide-Mullite-Alumina Nanocomposites. Journal of the American Ceramic Society, 1995, 78, 479-486.	3.8	62
574	Preparation of Fine Shirasuballoons from Vitric Volcaniclastic Materials Funtai Oyobi Fummatsu Yakin/Journal of the Japan Society of Powder and Powder Metallurgy, 1995, 42, 1128-1135.	0.2	11
575	Synthesis of LiSbO3 from Metal Alkoxides Funtai Oyobi Fummatsu Yakin/Journal of the Japan Society of Powder and Powder Metallurgy, 1995, 42, 603-607.	0.2	1
576	Zirconium-Hafnium Interdiffusion in Polycrystalline Fluorite-Cubic CeO2ZrO2HfO2 Solid Solution. Journal of the American Ceramic Society, 1993, 76, 1381-1383.	3.8	5

#	Article	IF	CITATIONS
577	Characterization of the Surface Oxide Layer of Iron Ultrafine Particles Nippon Kagaku Kaishi / Chemical Society of Japan - Chemistry and Industrial Chemistry Journal, 1993, 1993, 92-97.	0.1	3
578	Effects of cold isostatic pressure on the sintering behaviour of nickel ultrafine powders. Journal of Alloys and Compounds, 1992, 190, 31-33.	5.5	4
579	Oxidation and Degradation of Titanium Nitride Ultrafine Powders Exposed to Air. Journal of the American Ceramic Society, 1992, 75, 244-248.	3.8	37
580	Sintering characteristics of cobalt ultrafine powders. Journal of the Less Common Metals, 1991, 168, 277-287.	0.8	9
581	Cation Interdiffusion and Phase Stability in Polycrystalline Tetragonal Ceria-Zirconia-Hafnia Solid Solution. Journal of the American Ceramic Society, 1991, 74, 2610-2614.	3.8	64
582	Effects of cold isostatic pressures on the sintering behaviour of iron and copper ultrafine powders. Journal of Materials Science Letters, 1991, 10, 426-428.	0.5	5
583	Surface Phases of Iron Ultrafine Powders Estimated from Thermal Desorption Measurements and Their Reduction Characteristics. Nippon Kinzoku Gakkaishi/Journal of the Japan Institute of Metals, 1991, 55, 219-226.	0.4	14
584	Gas evolution characteristics of palladium ultrafine powders Funtai Oyobi Fummatsu Yakin/Journal of the Japan Society of Powder and Powder Metallurgy, 1990, 37, 508-512.	0.2	1
585	Gas adsorption and desorption characteristics of oxide superconducting powders Funtai Oyobi Fummatsu Yakin/Journal of the Japan Society of Powder and Powder Metallurgy, 1990, 37, 761-764.	0.2	2
586	Sintering and Gas Desorption Characteristics of Copper Ultrafine Powders. Materials Transactions, JIM, 1990, 31, 802-809.	0.9	10
587	Mechanical and magnetic properties of the rapidly quenched Cu2MnAl. Journal of Materials Science, 1990, 25, 2549-2556.	3.7	6
588	Sorption and Desorption Characteristics of Water Vapour on YBa2Cu3O7-xPowders. Japanese Journal of Applied Physics, 1990, 29, L2022-L2025.	1.5	6
589	Gas Evolution and Densification during Sintering of Ultrafine Copper Powders. Nippon Kinzoku Gakkaishi/Journal of the Japan Institute of Metals, 1989, 53, 422-428.	0.4	5
590	Synthesis and Characterization of the Mixed and the Composite Ni-TiN Utrafine Particles. , 1989, , 203-212.		0
591	Improvement of the hard magnetic properties in Mn-Al-X (X = C, Ti) systems by twin-roll quenching. Journal of Materials Science Letters, 1989, 8, 1123-1126.	0.5	0
592	Permanent deformation of (Co, Ni)Zr intermetallic compounds through phase transformation. Journal of Materials Science, 1989, 24, 2891-2897.	3.7	3
593	Reduction and sintering of ultrafine copper powders. Journal of Materials Science Letters, 1989, 8, 273-276.	0.5	5
594	Cation Interdiffusion in Polycrystalline Cubic C-Type Yttria-Zirconia-Hafnia Solid Solutions. Journal of the American Ceramic Society, 1989, 72, 2121-2125.	3.8	16

ΥΟSΗΙΟ SAKKA

#	Article	IF	CITATIONS
595	Low-temperature sintering and gas desorption of gold ultrafine powders. Journal of the Less Common Metals, 1989, 147, 89-96.	0.8	26
596	Sintering and Gas Release of Ag Ultrafine Powders. Nippon Kinzoku Gakkaishi/Journal of the Japan Institute of Metals, 1989, 53, 614-620.	0.4	15
597	Sintering of Copper Ultrafine Powders. , 1989, , 193-202.		Ο
598	Compressive deformation of CoZr and (Co,Ni)Zr intermetallic compounds with B2 structure. Journal of Materials Science, 1988, 23, 4041-4048.	3.7	40
599	Superconducting and Transport Properties of B-Y-Cu-O Compounds -Orthorhombic and Tetragonal Phases. Japanese Journal of Applied Physics, 1987, 26, L721-L723.	1.5	50
600	Enhancement of MgO Evaporation from MgO-Stabilized ZrO2 by Grain-Boundary Diffusion. Journal of the American Ceramic Society, 1986, 69, 111-113.	3.8	10
601	Cation Interdiffusion in Polycrystalline Fluorite-cubic MgO–ZrO2Solid Solution. Bulletin of the Chemical Society of Japan, 1982, 55, 420-422.	3.2	25
602	Preparation and Utilization of Fine Expanded Perlite. Key Engineering Materials, 0, 280-283, 701-706.	0.4	2
603	Fabrication of Highly Microstructure Controlled Ceramics by Novel Colloidal Processing. Key Engineering Materials, 0, 336-338, 2372-2377.	0.4	0
604	Rare-Earth-Dependent Magnetic Anisotropy in REBa ₂ Cu ₃ O _{<i>y</i>} . Applied Physics Express, 0, 1, 031701.	2.4	22
605	Pulsed-DC Electrophoretic Deposition (EPD) of Aqueous Alumina Suspension for Controlling Bubble Incorporation and Deposit Microstructure. Key Engineering Materials, 0, 412, 39-44.	0.4	10
606	Textured PbTiO ₃ Based Ceramics Fabricated by Slip Casting in a High Magnetic Field. Key Engineering Materials, 0, 421-422, 395-398.	0.4	0
607	Control of Residual Stress in Multilayered Alumina Composites Prepared Using EPD in a Strong Magnetic Field. Key Engineering Materials, 0, 412, 233-236.	0.4	1
608	Fabrication of Textured β-Si ₃ N ₄ and β-Sialon by Slip Casting in a Strong Magnetic Field and Reaction-Sintering. Key Engineering Materials, 0, 434-435, 5-8.	0.4	0
609	Textured Ti ₃ SiC ₂ by EPD in a Strong Magnetic Field. Key Engineering Materials, 0, 507, 15-19.	0.4	2
610	Structural Features and Color Tunable Photoluminescence of the Binary and Ternary Layered Rare-Earth Hydroxides of (Y,Ln) ₂ (OH) ₅ NO ₃ · <i>n</i> H& (Ln=Tb, Eu). Key Engineering Materials, 0, 544, 252-258.	lt;Sub>	;2
611	Preparation of Barium Titanate Nanoperticles with Necking Structure/Polymer Complex and their Dielectric Properties. Key Engineering Materials, 0, 582, 23-26.	0.4	0
612	Preparation of Ceramics/Polymer Film Capacitor Using Barium Titanate Nanoparticles with High Dielectric Property and their Dielectric Property. Key Engineering Materials, 0, 566, 54-58.	0.4	0

#	Article	IF	CITATIONS
613	Luminescence Behaviors of the New Upconversion Phosphors of Yb/Ho Co-Doped (Gd _{1-<i>x</i>} Lu _{<i>x</i>}) _{3(x=0.1-0.5) Garnet Solid Solutions. Key Engineering Materials, 0, 602-603, 1034-1038.}	b>4Al&l1	t;sub>5& <mark>lt</mark>)
614	Chemical Reactivity and Cathode Properties of LaCoO ₃ on Lanthanum Silicate Oxyapatite Electrolyte. Key Engineering Materials, 0, 616, 120-128.	0.4	10
615	Textured Beta-Sialon:Eu ²⁺ Phosphor Deposits Fabricated by Electrophoretic Deposition (EPD) Process within a Strong Magnetic Field: Preparation Process and Photoluminescence (PL) Properties Depending on Orientation. Key Engineering Materials, 0, 654, 268-273.	0.4	0
616	Fabrication of c-Axis-Oriented Zeolite L Seed Layer on Porous Zirconia Substrate by Electrophoretic Deposition in Strong Magnetic Field. Key Engineering Materials, 0, 654, 274-279.	0.4	0
617	Tri-axial Grain Orientation of Y ₂ Ba ₄ Cu ₇ O _{<i>y</i>} Achieved by the Magneto-science Method. Applied Physics Express, 0, 1, 111701.	2.4	46